Department for
Business, Energy
& Industrial Strategy

Endurance Well Injectivity Fracturing Study with REVEAL™

Key Knowledge Document

NS051-SS-REP-000-00017

August 2021

Acknowledgements

Any enquiries regarding this publication should be sent to us at:
enquiries@beis.gov.uk

Contents

1.0 Foreword

The Net Zero Teesside (NZT) project in association with the Northern Endurance Partnership project (NEP) intend to facilitate decarbonisation of the Humber and Teesside industrial clusters during the mid-2020s. Both projects will look to take a Final Investment Decision (FID) in early 2023, with first CO2 capture and injection anticipated in 2026.

The projects address widely accepted strategic national priorities – most notably to secure green recovery and drive new jobs and economic growth. The Committee on Climate Change (CCC) identified both gas power with Carbon Capture, Utilisation and Storage (CCUS) and hydrogen production using natural gas with CCUS as critical to the UK's decarbonisation strategy. Gas power with CCUS has been independently estimated to reduce the overall UK power system cost to consumers by £19bn by 2050 (compared to alternative options such as energy storage).

1.1 Net Zero Teesside Onshore Generation & Capture

NZT Onshore Generation & Capture (G&C) is led by bp and leverages world class expertise from ENI, Equinor, and TotalEnergies. The project is anchored by a world first flexible gas power plant with CCUS which will compliment rather than compete with renewables. It aims to capture ~2 million tonnes of CO2 annually from 2026, decarbonising 750MW of flexible power and delivering on the Chancellor's pledge in the 2020 Budget to "support the construction of the UK's first CCUS power plant." The project consists of a newbuild Combined Cycle Gas Turbine (CCGT) and Capture Plant, with associated dehydration and compression for entry to the Transportation & Storage (T&S) system.

1.2 Northern Endurance Partnership Onshore/Offshore Transportation & Storage

The NEP brings together world-class organisations with the shared goal of decarbonising two of the UK's largest industrial clusters: the Humber (through the Zero Carbon Humber (ZCH) project), and Teesside (through the NZT project). NEP T&S includes the G&C partners plus Shell, along with National Grid, who provide valuable expertise on the gathering network as the current UK onshore pipeline transmission system operator.

The Onshore element of NEP will enable a reduction of Teesside's emissions by one third through partnership with industrial stakeholders, showcasing a broad range of decarbonisation technologies which underpin the UK's Clean Growth strategy and kickstarting a new market for CCUS. This includes a new gathering pipeline network across Teesside to collect CO2 from industrial stakeholders towards an industrial Booster Compression system, to condition and compress the CO2 to Offshore pipeline entry specification.

Offshore, the NEP project objective is to deliver technical and commercial solutions required to implement innovative First-of-a-Kind (FOAK) offshore low-carbon CCUS infrastructure in the UK, connecting the Humber and Teesside Industrial Clusters to the Endurance CO2 Store in the Southern North Sea (SNS). This includes CO2 pipelines connecting from Humber and Teesside compression/pumping systems to a common subsea manifold and well injection site

at Endurance, allowing CO2 emissions from both clusters to be transported and stored. The NEP project meets the CCC's recommendation and HM Government's Ten Point Plan for at least two clusters storing up to 10 million tonnes per annum (Mtpa) of CO2 by 2030.

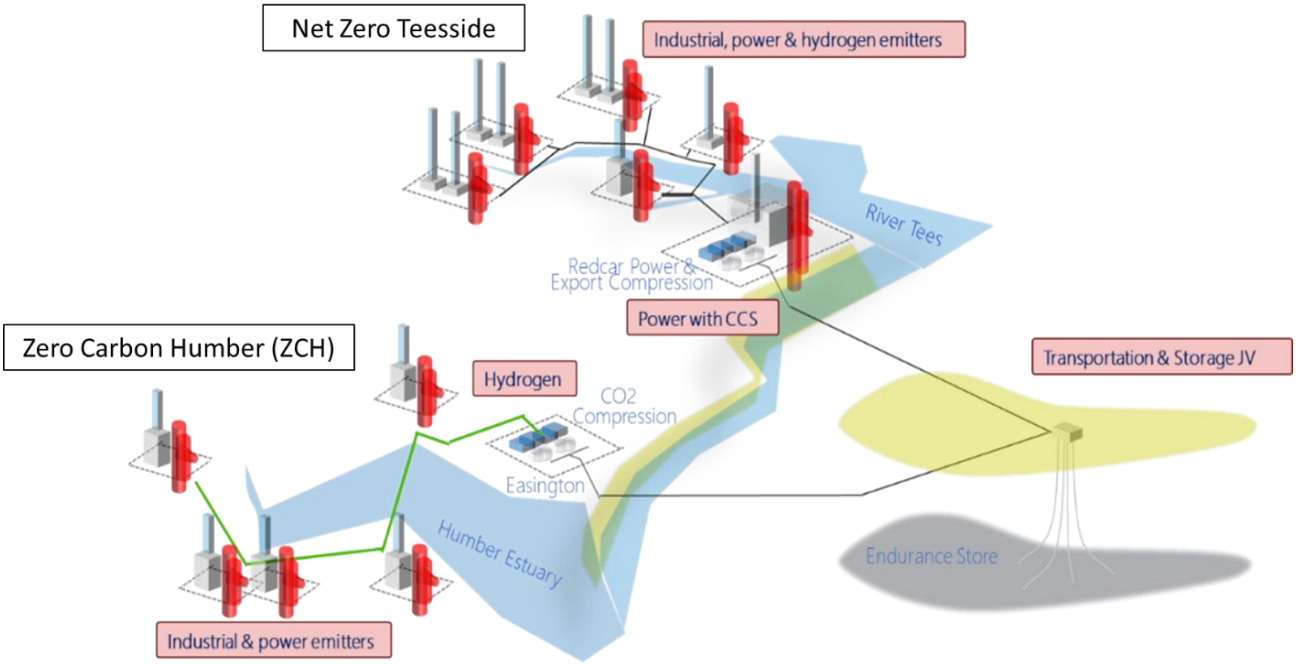

Figure 1: Overview of Net Zero Teesside and Zero Carbon Humber projects.

The project initially evaluated two offshore CO2 stores in the SNS: 'Endurance', a saline aquifer formation structural trap, and 'Hewett', a depleted gas field. The storage capacity requirement was for either store to accept 6+ Mtpa CO2 continuously for 25 years. The result of this assessment after maturation of both options, led to Endurance being selected as the primary store for the project. This recommendation is based on the following key conclusions:

- The storage capacity of Endurance is 3 to 4 times greater than that of Hewett
- The development base cost for Endurance is estimated to be 30 to 50% less than Hewett
- CO2 injection into a saline aquifer is a worldwide proven concept, whilst no benchmarking is currently available for injection in a depleted gas field in which Joule-Thompson cooling effect has to be managed via an expensive surface CO2 heating solution.

Following selection of Endurance as the primary store, screening of additional stores has been initiated to replace Hewett by other candidates. Development scenarios incorporating these additional stores will be assessed as an alternative to the sole Endurance development.

2.0 Symbols and Abbreviations

For this document the following symbols and abbreviations apply:

MTPA	Millions metric Tons of CO2 per Annum (~52 mmscfd)
mmscfd	Millions of standard cubic feet per day

3.0 Executive Summary

The purpose of the study was to use the REVEAL™ reservoir simulation package, with its unique fracture modelling capabilities, to determine the likelihood of having poor conformance or low injectivity risks during the injection of cool CO2 into the Endurance CCS storage reservoir.

More specifically, these risks are:

1) that a thermally induced fracture might extend vertically to the top of the Bunter sandstone, with a possible impact on the maximum allowed operating pressure.
2) that there is insufficient injectivity at the maximum allowed bottom hole pressure, to achieve the required CO2 injection rate.
3) that, for the required injection rate, the bottom hole pressure approaches its safe limit leading to rate curtailment.
4) that thermally induced fracturing will cause poor injection conformance, either within or beyond the perforated interval, leading to inefficient use of the storage volume.

Risks (1), (2) and (3) all refer to the ability to inject the required volume.

The results of the study have indicated the following:

- The Risk of vertical fracture growth is manageable and low based upon screened tested cases:
    - No case presents fracture reaching top Bunter by the end of injection
    - The study has demonstrated the value of leaving a section of the Bunter unperforated (at least 20-30 meters), both for pressure limit and conformance
- Skin build-up (and associated injectivity loss) is likely to be offset by thermal fracturing. In the low probability case where fracturing does not occur and there is formation damage (case #4/V37 with low Young's Modulus and high skin), late life BHP could require curtailment due to WDOL pressure limit for the crestal well. This indicates the importance of avoiding high skin in order to achieve acceptable injection rate across the full uncertainty range. Further assurance on Young's modulus would help, for example

from quantitative analysis of the 2013 water injection test in 42/25d-3, in which fracturing did occur.

- Thermal fracturing is not adversely impacting the confinement of CO2 plume movement. In particular, there appears to be a low risk of CO2 moving vertically through a fracture to top reservoir. The potential low kv/kh system (well 42/25d-3 PTA interpretation) would support longer perforated interval i.e. 80 meters. The well is unlikely to thermally fracture immediately hence maintaining good conformance over the initial period.

4.0 Introduction

The purpose of the study carried out by Carbon Fluids Ltd Consultancy was to use the REVEAL™reservoir simulation package (part of the IPM suite of tools produced by Petroleum Experts Limited of Edinburgh, UK) with its unique fracture modelling capabilities, to determine the likelihood of certain risks occurring during the injection of cool CO2 into the Endurance CCS storage reservoir.

These risks are:

1) that a thermally induced fracture might extend vertically to the top of the Bunter sandstone, with a possible impact on the maximum allowed operating pressure.
2) that there is insufficient injectivity, at the maximum allowed bottom hole pressure, to achieve the required CO2 injection rate.
3) that, for the required injection rate, the bottom hole pressure approaches its safe limit, leading to rate curtailment.
4) that thermally induced fracturing will cause poor injection conformance leading to inefficient use of the storage volume.

Risks (1), (2) and (3) refer to the ability to inject the required volume.

The first part of the work was to develop a REVEAL™ model equivalent to the Nexus® reservoir simulation model used to develop a full field model (FFM) of the Endurance storage reservoir. As Nexus® is an isothermal code it is not capable of modelling thermal effects. It is not capable of modelling thermal fracturing. The FFM developed in REVEAL™ was then reduced to a sector model, with boundary conditions which allowed it to simulate the FFM in terms of pressure and gas saturation.

A base case sector model was defined using geo-mechanical properties derived from the geo-mechanical study carried out in Visage™. The fracture option in REVEAL™ was then used to simulate the effects of a thermally induced fracture in one of the wells.

A sensitivity study was performed by varying the parameters in the base case REVEAL™ model in a series of simulations. An analysis of the results enabled conclusions to be drawn about the likelihood of the occurrence of the risks listed above.

5.0 Description of the Modelling Workflow

A slightly reduced version of the Nexus® grid and its properties (NTG, porosities and permeabilities, as well as its saturation functions) was read into REVEAL™ to create a clone model. Using the same wells' schedule as the Nexus® simulation, REVEAL™ was run, and the reservoir pressure and gas saturations were compared with those from Nexus®. The comparison showed that REVEAL™ produced results which were acceptably close to those from Nexus®.

Figure 2 shows a comparison of the Nexus® and REVEAL™ reservoir pressures versus time, for the injection period. Output from an isothermal version of REVEAL™ is shown. Nexus® is an isothermal-only code and an isothermal version of REVEAL™ is the appropriate comparison to make.

In both models, each of the five injection wells injects 0.75 MMTPA of CO2 for 25 years, from January 2025 to January 2050.

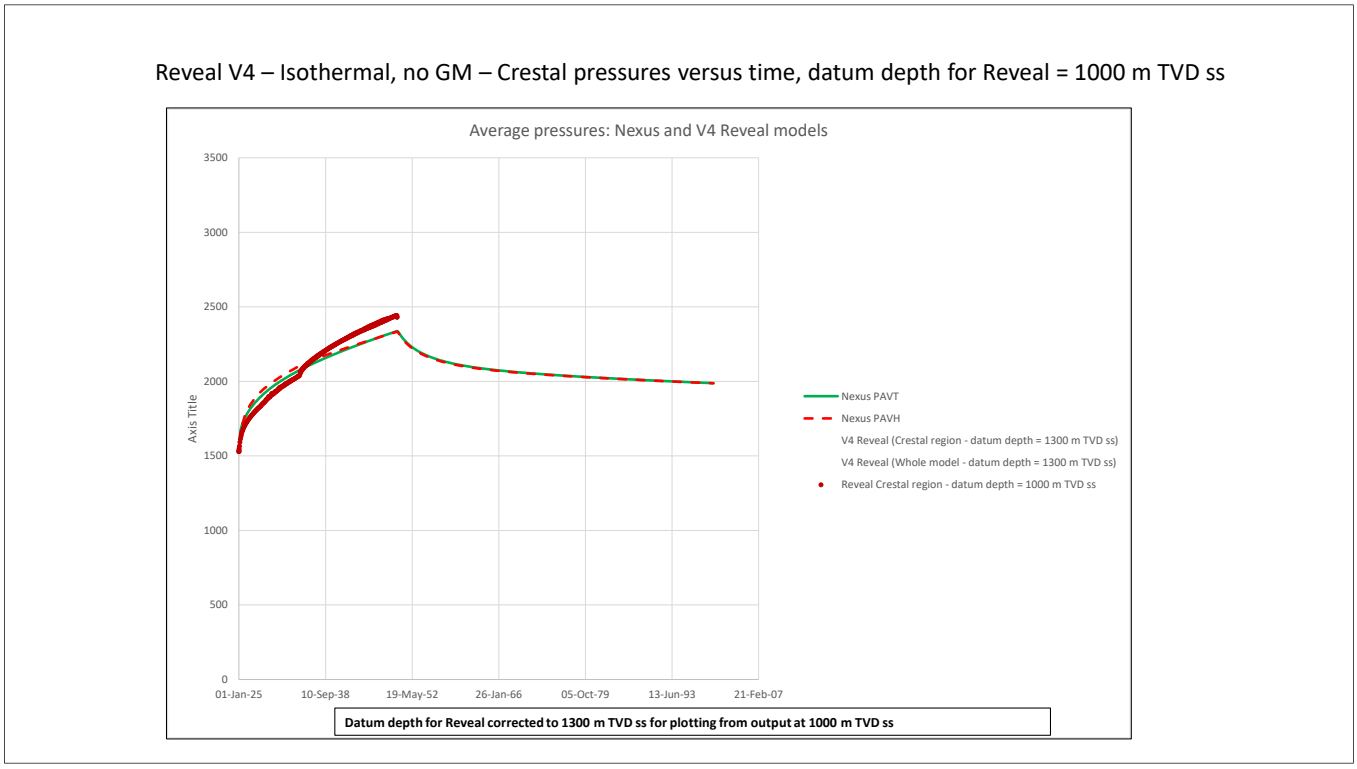

Figure 2: Reservoir pressures from Nexus® and an isothermal version of REVEAL™

The next stage in the work was to reduce the long run times of the REVEAL™ model by adopting a sector (small scale) model which would run quickly but retain the essential components of the simulation.

Figure 3 shows the relationship between the sector model grid and the FFM grid. The boundaries of the sector model are shown as the red box. The boundary cells of the sector model were given pore volume multipliers to create an equivalent pore volume to the FFM. This ensured a similar pressure response from the two models.

The Reveal FFM and Sector model grids

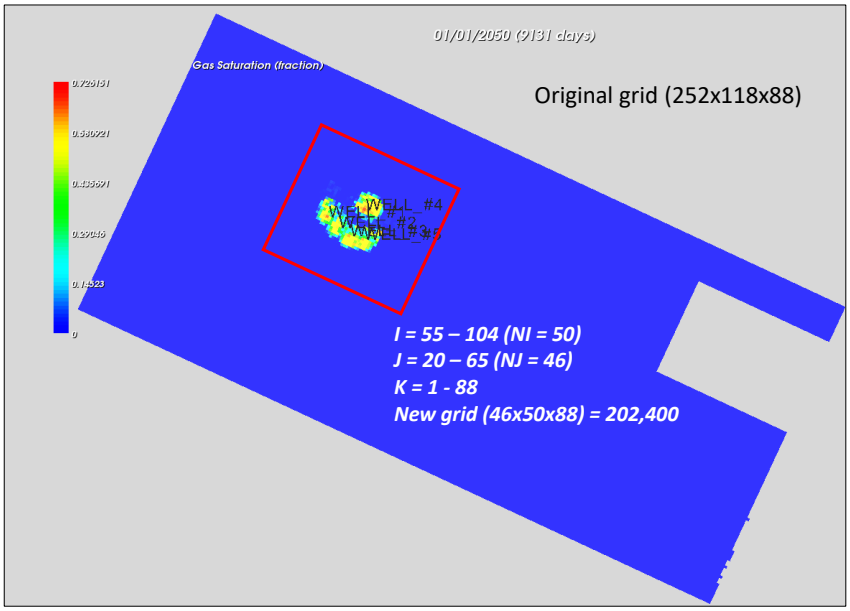

Figure 3: The REVEAL™ FFM and Sector (red outline in figure) model grids.

Figure 4 shows a comparison of the Nexus® FFM, two versions of the REVEAL™ FFM (V4 – isothermal and V5 – thermal), and the REVEAL™ sector model (V7 – thermal and with the geo-mechanical option). The resulting reservoir pressures are similar, and the sector model was deemed to be an acceptable representation of the full field models.

Comparison of pressure versus time in Crestal region; Nexus, Reveal (V4 – isothermal, no GM), (V5 – thermal, no GM), (V7 – small, thermal + GM)

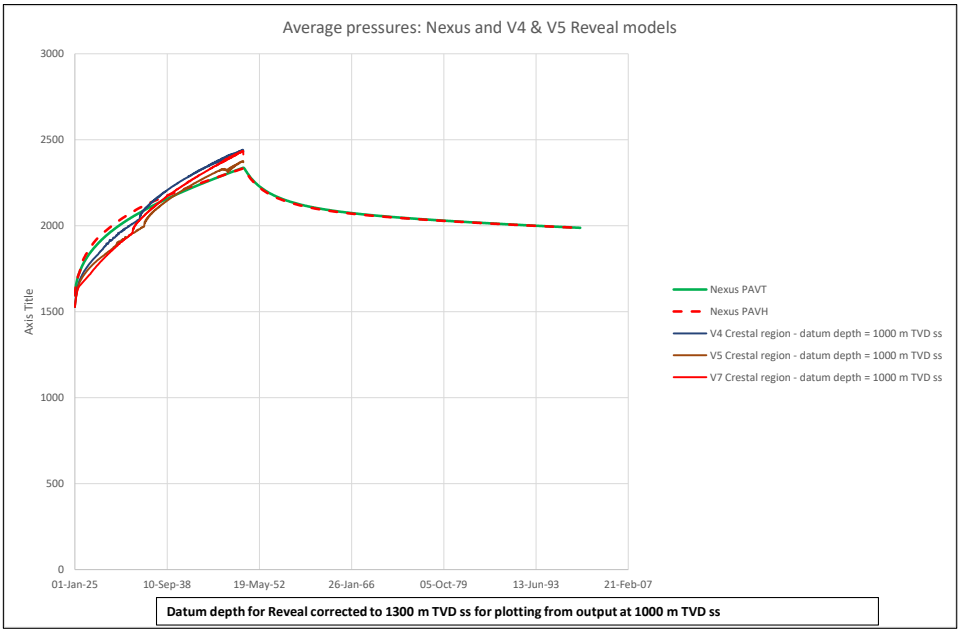

Figure 4: Comparison of reservoir pressures from the Nexus® FFM, 2 versions of the REVEAL™ FFM and the REVEAL™ sector model

Figure 5 to Figure 10 compare the REVEAL™ FFM and sector models in terms of gas saturation (Figure 5), dissolved CO2 (Figure 6), pressure (Figure 7), pressure change over initial pressure (

Figure **8**), temperature (Figure 9) and effective minimum horizontal stress (Figure 10).

V5 – Thermal , no GM – GAS SATURATION - end of injection (1 Jan 2050)

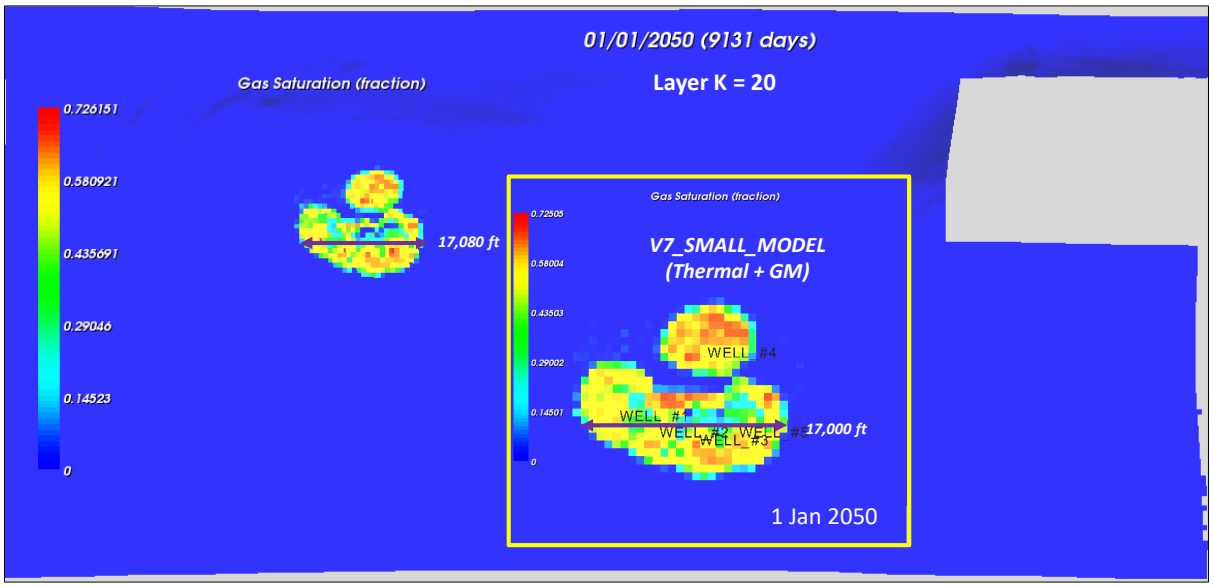

3x vertical exaggeration

Figure 5: Comparing gas saturations in the REVEAL™ FFM and sector models

V5 – Thermal, no GM – DISSOLVED CO_2 - end of injection (1 Jan 2050)

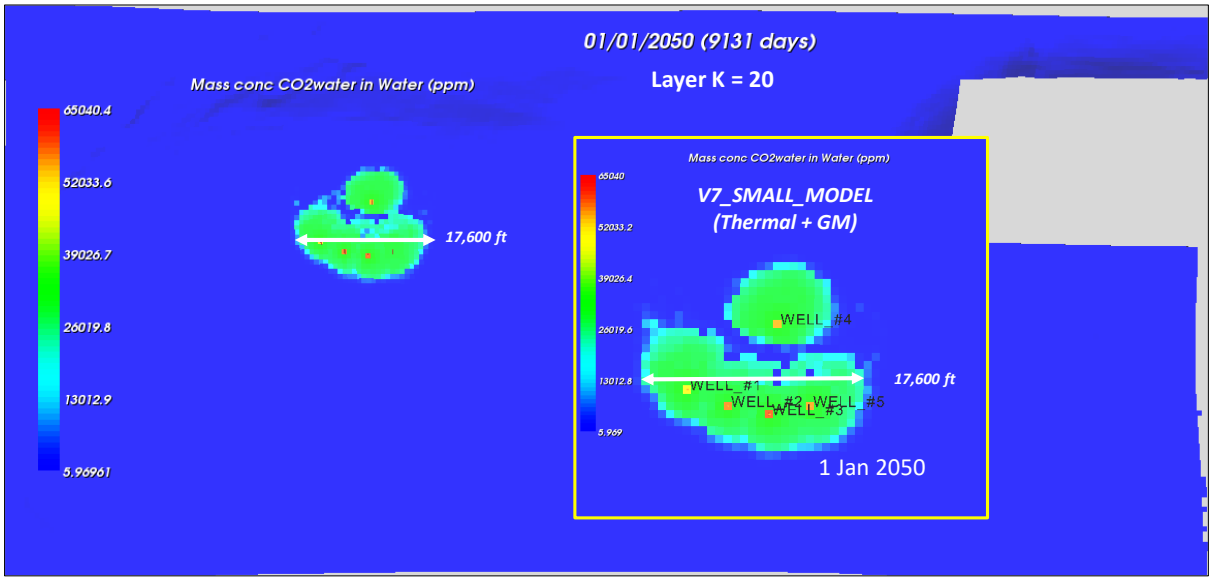

3x vertical exaggeration

Figure 6:Comparing dissolved CO2 concentrations in the REVEAL™ **FFM and sector models**

V5 – Thermal, no GM – PRESSURE - end of injection (1 Jan 2050)

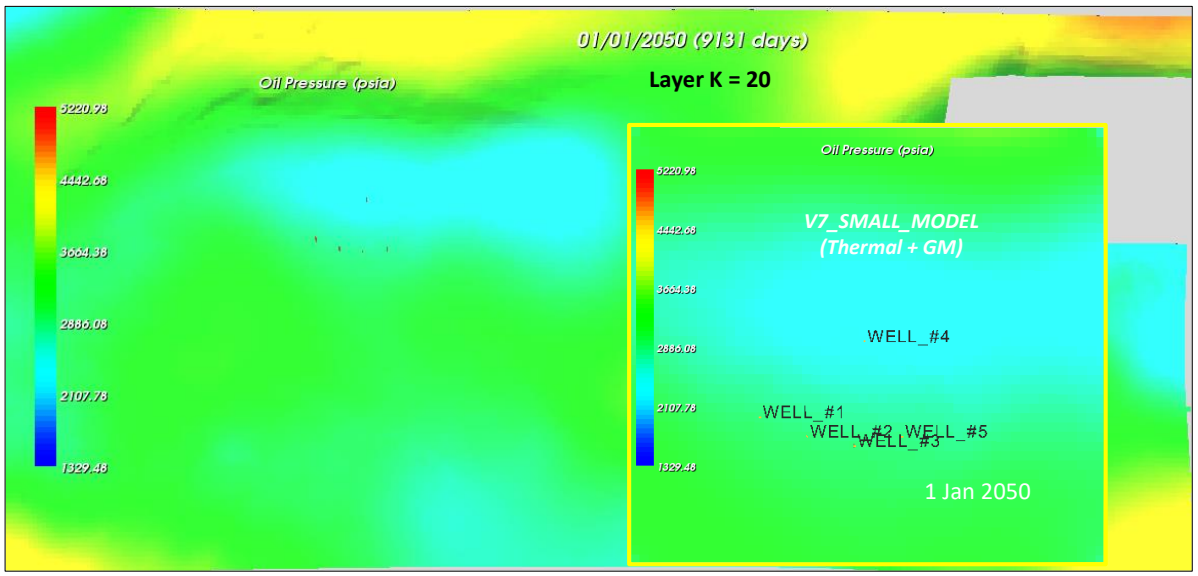

3x vertical exaggeration

Figure 7: Comparing gas pressures in the REVEAL™ FFM and sector models

V5 – Thermal, no GM – dP = (Pressure (1 Jan 2050) – Initial Pressure)

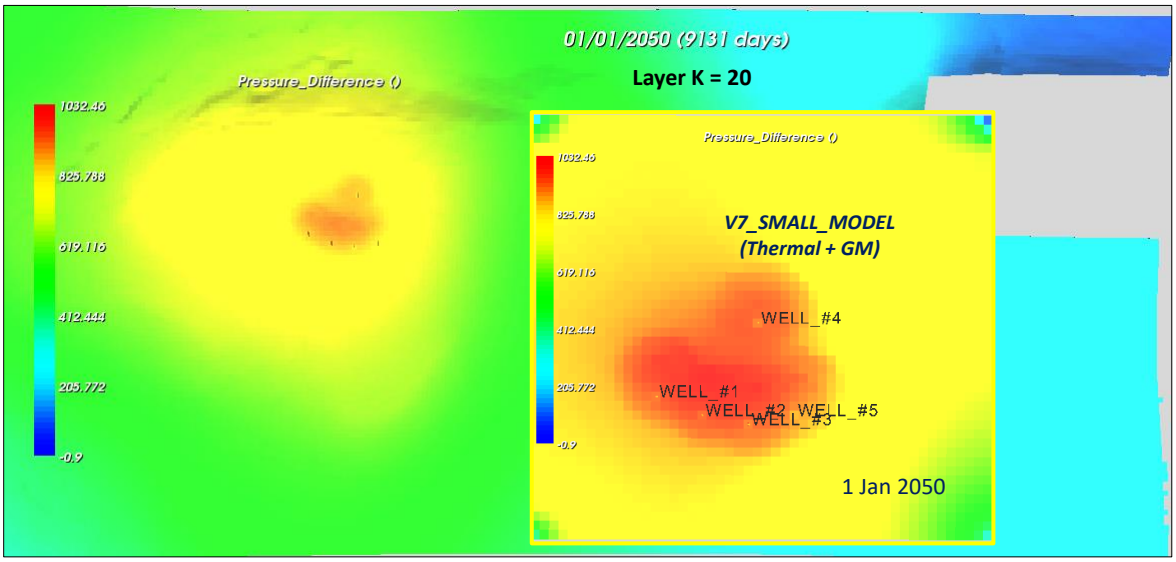

3x vertical exaggeration

Figure 8: Comparing the change in pressure in the REVEAL™ FFM and sector models

V5 – Thermal, no GM – Temperature (ºC)

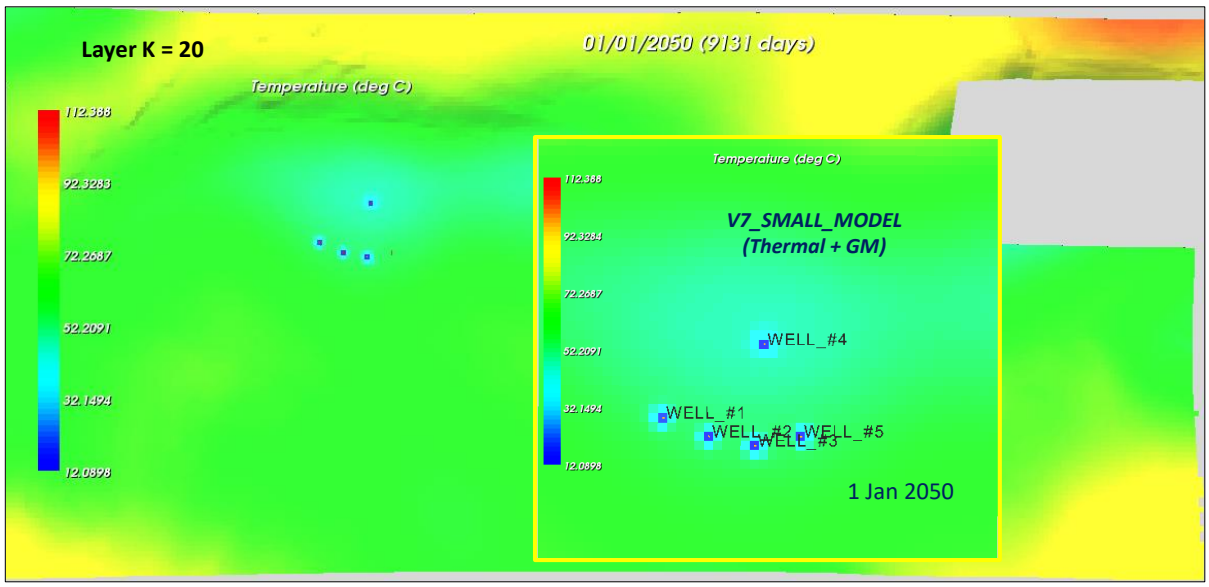

3x vertical exaggeration

Figure 9: Comparing temperatures in the REVEAL™ FFM and sector models

V6 – Thermal , plus GM – Effective STRESSX - (Jan 2050 – end of injection)

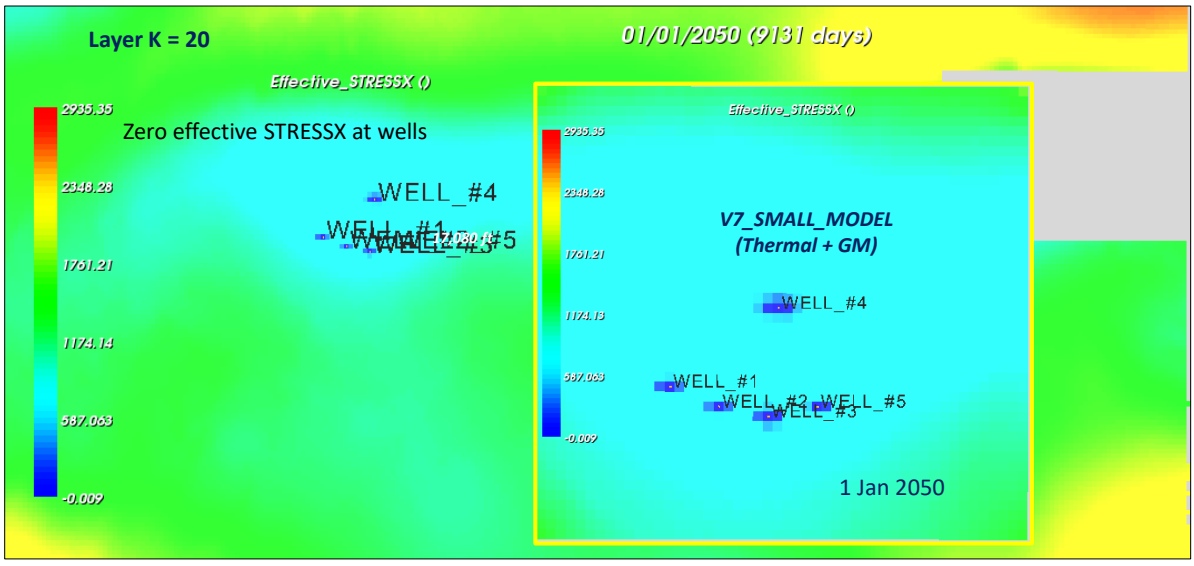

3x vertical exaggeration

Figure 10: Comparing effective minimum horizontal stresses in the REVEAL™ FFM and sector models

These results were taken to show that the sector model was an adequate model for the study.

6.0 Base Case

The geo-mechanical properties for the base case (V14) are shown in Table 1.

Base case geo-mechanical properties

Parameter	Value chosen	Source
Young's modulus	1.61E6 psi	Bunter s/s All table (mid)
Poisson's ratio	0.22	Bunter s/s All table (mid)
Biot's coefficient	0.7	Assumed
Linear thermal expansion coefficient	1.5E-5 1/degC	Assumed
X-direction stress gradient	0.778 psi/ft	Bunter s/s All table (mid)
Y-direction stress gradient	0.807 psi/ft	Ratio Shmax:Shmin stress Bunter s/s All table
Z-direction stress gradient	1.02 psi/ft	Ratio Sv:Shmin stress Bunter s/s All table
Poro-elastic coefficient	2.43E-7 1/psi	Calculated
Thermo-elastic coefficient	24.8 psi/deg C	Calculated

*Poros-elastic coeff = (Biot coeff *(1- 2*PR))/YM*
*Thermo-elastic coeff = Linear therm exp coeff * YM / (1 – PR)*

Table 1: Base case geo-mechanical properties derived from the Endurance Geomechanical model (VisageTM).

The critical stress intensity was set to zero. Previous experience has shown that this is not a critical factor once the fracture has started to grow. The well selected for the fracturing test was the crestal well, well #4, in the simulation model.

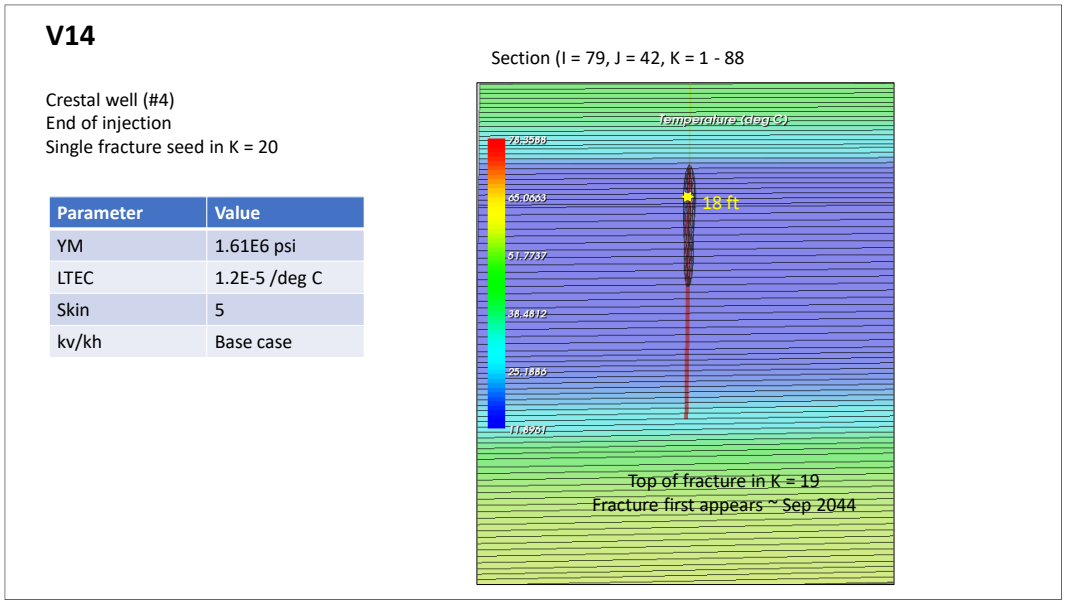

Figure 11: Temperature profile and fracture plot for the base case run at the end of injection.

Figure 11 and Figure 12 show the resulting fracture at the end of injection within a plot of temperature and gas saturation for a vertical column of cells containing the well.

V14

Crestal well (#4)
End of injection
Single fracture seed in K = 20

Parameter	Value
YM	1.61E6 psi
LTEC	1.2E-5 /deg C
Skin	5
kv/kh	Base case

Model stops with NaN in 2034 when
All wells have Skin = 5
Re-run with crestal well with Skin =5
Other wells, Skin = 0

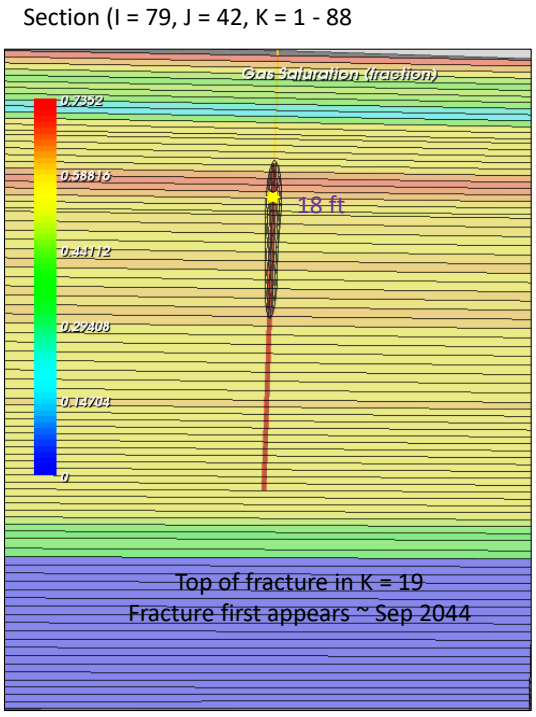

Figure 12: Gas saturation profile and fracture plot for the base case run at the end of injection

V14

Crestal well (#4)
End of injection
Single fracture seed in K = 20

Parameter	Value
YM	1.61E6 psi
LTEC	1.2E-5 /deg C
Skin	5
kv/kh	Base case

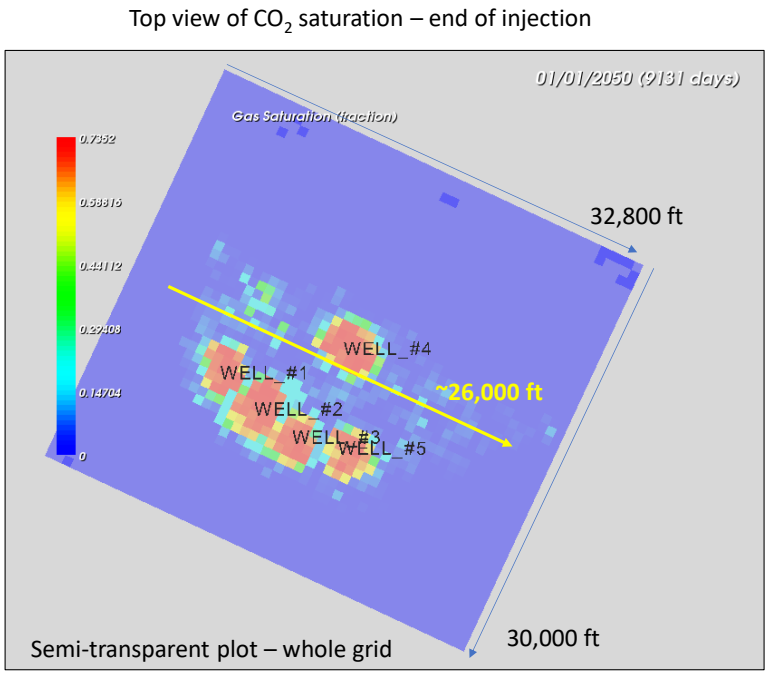

Figure 13: Gas saturation, top view of whole sector model, for the base case run at the end of injection

Figure 13 shows a semi-transparent plot of a top view of gas saturation at the end of injection for the whole sector model. Figure 14 shows a plot of the well's BHP, the reservoir pressure, injectivity and the safe maximum BHP. The upper safe pressure limit for the crestal well #4 was defined as 3250 psia at a datum depth of 1300 m TVD ss (USOL set to 204 bars at 1020m TVDss + (1300-1020)/0.3048 * 0.32).

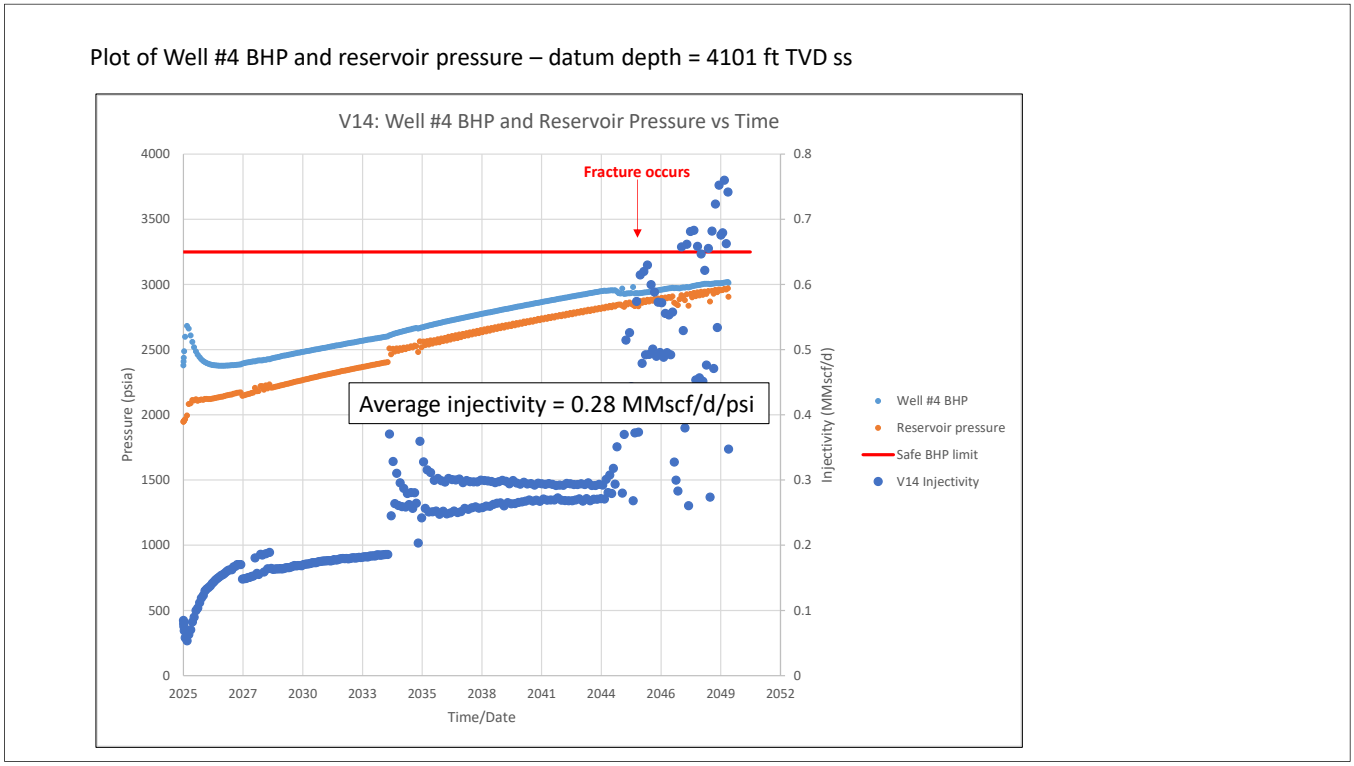

Figure 14: Well #4 BHP, reservoir pressure, injectivity and safe BHP limit

The effect of the occurrence of a fracture can clearly be seen in the plot of injectivity. All the wells were able to inject at their required rates for the required injection period.

Figure 15 and Figure 16 show cross sections through the model of gas saturations and temperature at the end of injection.

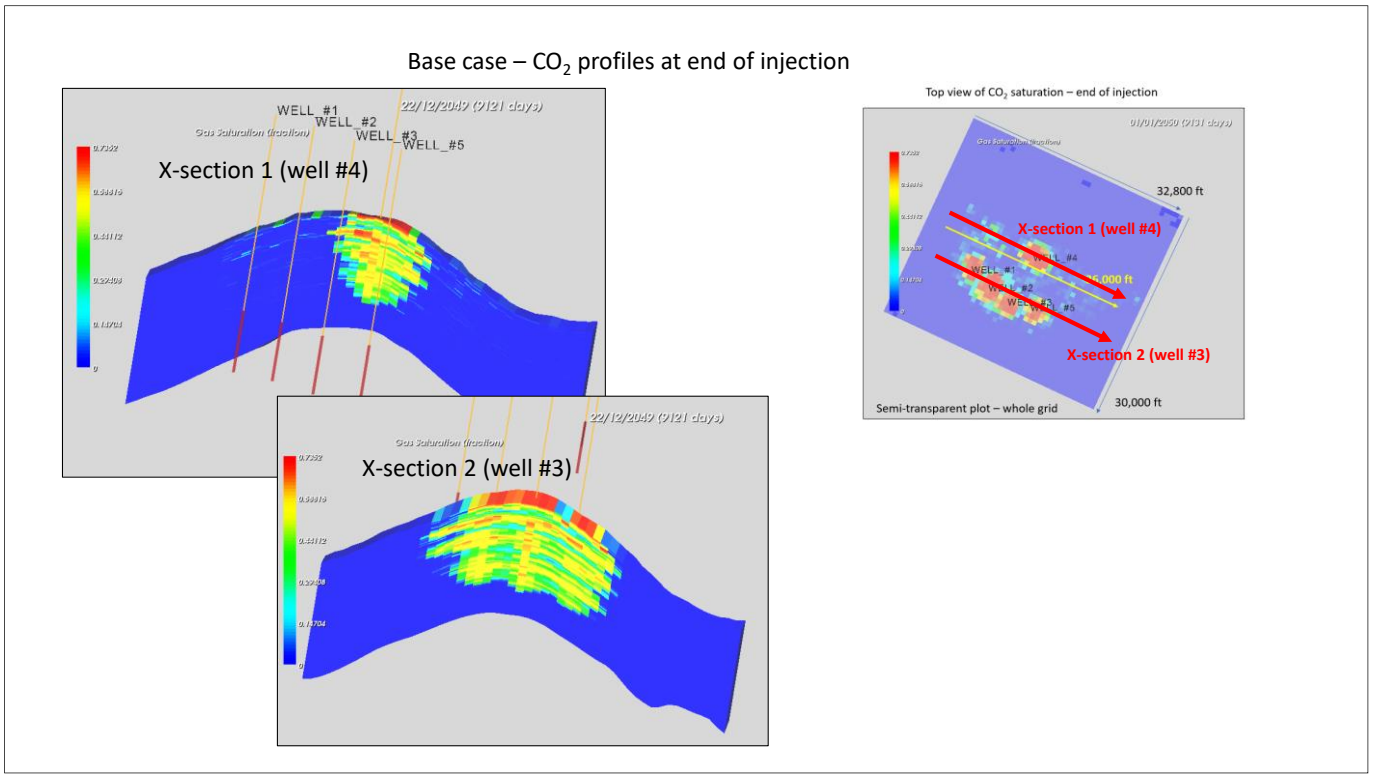

Figure 15: Base case gas saturation profiles at the end of injection

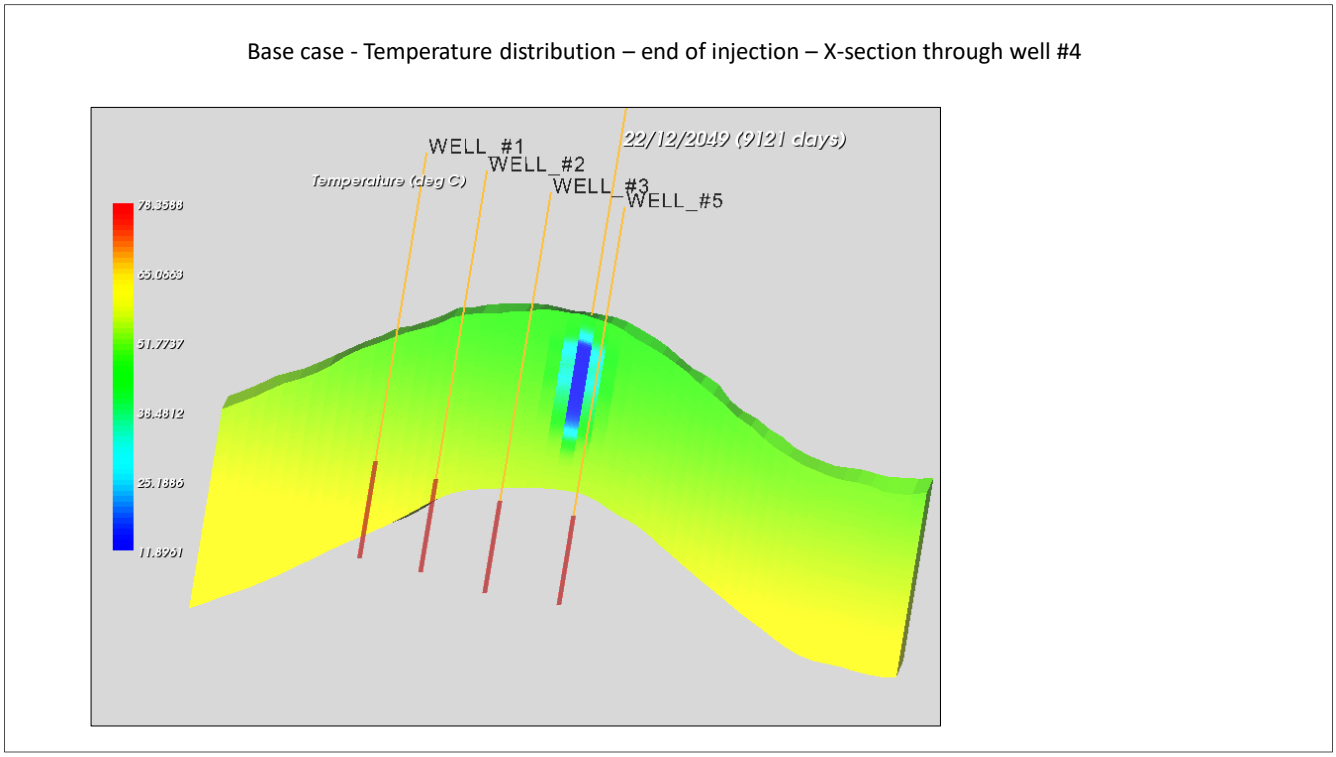

Figure 16: Base case temperature profile at the end of injection

Figure 17 shows the how the pressure gradient across the fracture was calculated.

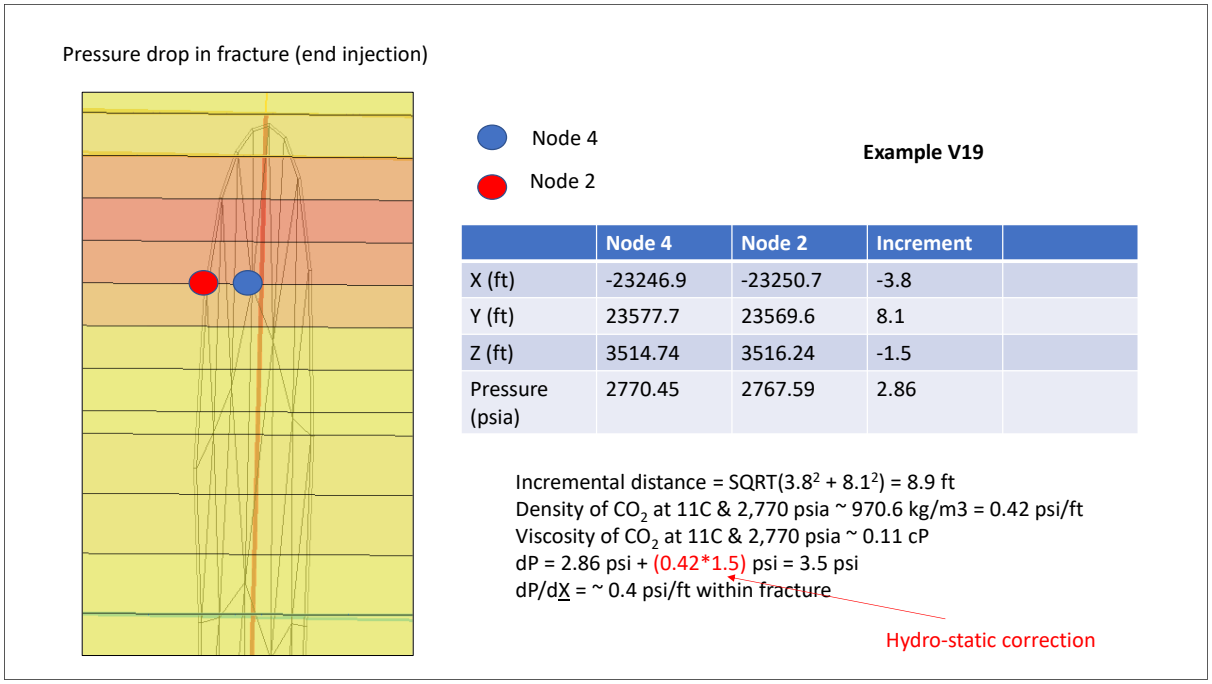

	Node 4	Node 2	Increment	
X (ft)	-23246.9	-23250.7	-3.8	
Y (ft)	23577.7	23569.6	8.1	
Z (ft)	3514.74	3516.24	-1.5	
Pressure (psia)	2770.45	2767.59	2.86	

Figure 17: Calculating the pressure gradient across the fracture

Following the successful run of the base case, a series of sensitivity runs were made to determine the effect of changing the values of key parameters on the likelihoods of the risked events occurring.

7.0 Sensitivity Study

Table 2 lists the parameters which were varied in the sensitivity study, along with their values.

Principal parameters tested

Parameter	Low value	Mid value	High value	Large value
Young's modulus	0.8E-6 psi	1.61E6 psi	3.2E6 psi	
Linear thermal expansion coefficient		1.2E-5 $^{o}C^{-1}$	1.5E-5 $^{o}C^{-1}$	
kv/kh ratio	Low	Base	High	
Degree of cementation above injection well	None	Base		
Well skin	0	5	30	
Pore volume connected to injection well	Low (1/2 Base)	Base		
Number of places fractures could starts (fracture seeds)	0 (no fracture)	1	2	3
Biot coefficient		0.7	1.0	
Fracture conductivity	0.1 D ft	1.0 D ft		

Table 2: Parameters tested in sensitivity study, and values

A total of 31 simulation were run to determine the sensitivity of the results to changes in these parameters. **Table 3** lists the runs and their properties:

- **V11 – V18 (8 runs)** – These tested three parameters; the Young's modulus (mid and high values); the linear thermal expansion coefficient (LTEC) (mid and high values); and the kv/kh ratio (mid and high values). V14 was the Base Case.

Note that when we refer to the kv/kh value, it is shorthand for changing the geological description (the porosity, permeability and net-to-gross values) of the model.

- **V19** – This was a run of the base case but with no cemented (reduced porosity and permeability caused by diagenesis) above the perforated interval.
- **V20** – V23 (4 runs) – These were runs to test the effect of changing the skin values for the injection well, with mid and high case kv/kh ratios.
- **V24** – V29 (6 runs) – These runs tested the effect of removing the fracture option – so a no-fracture run.
- **V30** – V31 (2 runs) – These tested the effects of adding extra fracture seeds, i.e. points where very small initial fractures are set to see if a fracture will grow.

- **V32** – A run with reduced connected pore volume. This was achieved by setting the pore volume multipliers on the boundary of the grid to half their base case values.
- **V33** – V34 (2 runs) – These were designed to be worst case examples. In V33, kv/kh and the well skin took their high values and the cemented region above the perforations was replaced by a more permeable zone (using the properties of the nearest uncemented layer). The connected pore volume took its low case value. The Young's modulus, LTEC took their LOW values. V34 was a copy of V33, except that Young's modulus and the LTEC took their HIGH values.
- **V35** – This was a copy of V34 but well #1 was shut-in and the injection rate for the crestal well was increased from 0.75 MMTPA to 1.0 MMTPA, to model a case where the crestal well has to make-up some of the injection rate from a failed off-crest injection well (well #1 in this case).
- **V36** – This was a copy of the base case (V14) but with the injection rate for the crestal well increased from 0.75 MMTPA to 1.0 MMTPA, to model a case where the crestal well has to make-up some of the injection rate from a failed off-crest injection well (well #1 in this case).
- **V37** – V38 (2 runs) – These were copies of the base case (V14), but with Young's modulus was set to its LOW value (8.0E% psi) and the LTEC was set to its mid (base case) value. The skin was set to 30 in V37 and to 5 in V38.
- **V39** – A copy of the base case but with fracture conductivity reduced by a factor of 10 from 1.0 D ft to 0.1 D ft.
- **V40** – This was a copy of the base case (V14) but with the Biot coefficient set to 1.0, instead of 0.7.
- **V41** – This was the base case with the kv/kh ratio set to its LOW value.

In all cases the simulations were run to January 2055, 5 years after injection stopped to see if there were any fracture growth after injection ceased: none was observed. **Table 3** and Table 4 list the key results i.e.:

- Fracture length at the end of the injection period
- The shallowest layer reached by the fracture
- The time at which fracture growth started
- The average injectivity

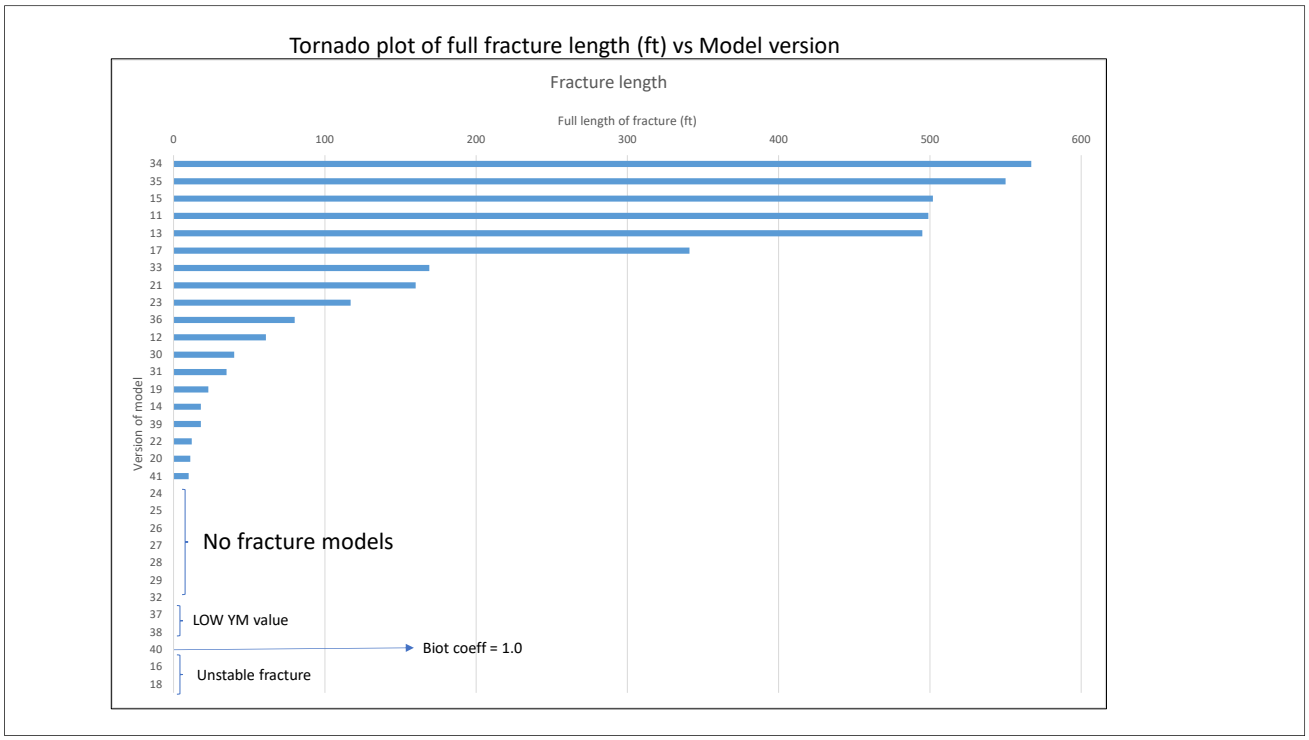

Figure 18 to Figure 24 show Tornado diagrams with respect to the reference case (V14) for full fracture length, change in injectivity, topmost layer reached by fracture, change in start time of fracture.

Table 3 – part 1

BP_SMALL_MODEL		GM Parameters																	
		Parameters to vary				Constant parameters													
	Model Version	Young's modulus	Linear thermal expansion coeficient	Skin	kv/kh ratio	Poisson's ratio	Biot's coefficient	Critical stress intensity	X-direction stress; offset	X-direction stress; gradient	Y-direction stress; offset	Y-direction stress; gradient	Z-direction stress; offset	Z-direction stress; gradient	Stress reversibility	Fracture model	Fracuring occurred
		psi	1/deg C			dimensionless	dimensionless	psi ($ft^{1/2}$)	psia	psi/ft	psia	psi/ft	psia	psi/ft			
	V11, single fracture seed, top perf, YM HIGH, LTE HIGH + 5 years	**3.20E+06**	**1.50E-05**	**5**	Base case	0.22	0.67	**0**	14.696	0.778	14.696	0.807	14.696	1.02	100%	ON	YES
	V12, single fracture seed, top perf, YM LOW, LTE HIGH + 5years	**1.61E+06**	**1.50E-05**	**5**	Base case	0.22	0.67	**0**	14.696	0.778	14.696	0.807	14.696	1.02	100%	ON	YES
	V13, single fracture seed, top perf, YM HIGH, LTE LOW + 5 years	**3.20E+06**	**1.20E-05**	**5**	Base case	0.22	0.67	**0**	14.696	0.778	14.696	0.807	14.696	1.02	100%	ON	YES
Reference Case	V14, single fracture seed, top perf, YM LOW, LTE LOW + 5 years	**1.61E+06**	**1.20E-05**	**5**	Base case	0.22	0.67	**0**	14.696	0.778	14.696	0.807	14.696	1.02	100%	ON	YES
	V15, single fracture seed, top perf, YM HIGH, LTE HIGH + 5 years	**3.20E+06**	**1.50E-05**	**5**	**High case**	0.22	0.67	**0**	14.696	0.778	14.696	0.807	14.696	1.02	100%	ON	YES
	V16, single fracture seed, top perf, YM LOW, LTE HIGH + 5 years	**1.61E+06**	**1.50E-05**	**5**	High case	0.22	0.67	**0**	14.696	0.778	14.696	0.807	14.696	1.02	100%	ON	YES
	V17, single fracture seed, top perf, YM HIGH, LTE LOW + 5 years	**3.20E+06**	**1.20E-05**	**5**	High case	0.22	0.67	**0**	14.696	0.778	14.696	0.807	14.696	1.02	100%	ON	YES
	V18, single fracture seed, top perf, YM LOW, LTE LOW + 5 years	**1.61E+06**	**1.20E-05**	**5**	High case	0.22	0.67	**0**	14.696	0.778	14.696	0.807	14.696	1.02	100%	ON	YES
Base case + NO cement above perfs	No cement above perforations, V19, single fracture seed, top perf, YM LOW, LTE LOW + 5 years	**1.61E+06**	**1.20E-05**	**5**	Base Case	0.22	0.67	**0**	14.696	0.778	14.696	0.807	14.696	1.02	100%	ON	YES
Base case with skin = 0 + fracture	V20, single fracture seed, top perf, YM LOW, LTE LOW + 5 years	**1.61E+06**	**1.20E-05**	**0**	**Base Case**	0.22	0.67	**0**	14.696	0.778	14.696	0.807	14.696	1.02	100%	ON	YES
Base case with skin = 30 + fracture	V21, single fracture seed, top perf, YM LOW, LTE LOW + 5 years	**1.61E+06**	**1.20E-05**	**30**	Base Case	0.22	0.67	**0**	14.696	0.778	14.696	0.807	14.696	1.02	100%	ON	YES
High kv/kh case with skin = 0 + fracture	V22, single fracture seed, top perf, YM LOW, LTE LOW + 5 years	**1.61E+06**	**1.20E-05**	**0**	High case	0.22	0.67	**0**	14.696	0.778	14.696	0.807	14.696	1.02	100%	ON	YES
High kv/kh case with skin = 30 + fracture	V23, single fracture seed, top perf, YM LOW, LTE LOW + 5 years	**1.61E+06**	**1.20E-05**	**30**	High case	0.22	0.67	**0**	14.696	0.778	14.696	0.807	14.696	1.02	100%	ON	YES
Base case with skin = 0 + NO fracture	V24, single fracture seed, top perf, YM LOW, LTE LOW + 5 years	**1.61E+06**	**1.20E-05**	**0**	**Base Case**	0.22	0.67	**0**	14.696	0.778	14.696	0.807	14.696	1.02	100%	**OFF**	n/a
Base case with skin = 5 + NO fracture	V25, single fracture seed, top perf, YM LOW, LTE LOW + 5 years	**1.61E+06**	**1.20E-05**	**5**	Base Case	0.22	0.67	**0**	14.696	0.778	14.696	0.807	14.696	1.02	100%	OFF	n/a
Base case with skin = 30 + NO fracture	V26, single fracture seed, top perf, YM LOW, LTE LOW + 5 years	**1.61E+06**	**1.20E-05**	**30**	Base Case	0.22	0.67	**0**	14.696	0.778	14.696	0.807	14.696	1.02	100%	OFF	n/a

List of sensitivity simulations

Table 3 – part 2

High kv/kh case with skin = 0 + NO fracture	V27, single fracture seed, top perf, YM LOW, LTE LOW + 5 years	1.61E+06	1.20E-05	0	High case	0.22	0.67	0	14.696	0.778	14.696	0.807	14.696	1.02	100%	OFF	n/a
High kv/kh case with skin = 5 + NO fracture	V28, single fracture seed, top perf, YM LOW, LTE LOW + 5 years	1.61E+06	1.20E-05	5	High Case	0.22	0.67	0	14.696	0.778	14.696	0.807	14.696	1.02	100%	OFF	n/a
High kv/kh case with skin = 30 + NO fracture	V29, single fracture seed, top perf, YM LOW, LTE LOW + 5 years	1.61E+06	1.20E-05	30	High case	0.22	0.67	0	14.696	0.778	14.696	0.807	14.696	1.02	100%	OFF	n/a
Base case + 2 fracture seeds	V30, 2x fracture seeds, top perf, YM LOW, LTE LOW + 5 years	1.61E+06	1.20E-05	5	Base Case	0.22	0.67	0	14.696	0.778	14.696	0.807	14.696	1.02	100%	ON	n/a
Base case + 3 fracture seeds	V31, 3x fracture seeds, top perf, YM LOW, LTE LOW + 5 years	1.61E+06	1.20E-05	5	Base Case	0.22	0.67	0	14.696	0.778	14.696	0.807	14.696	1.02	100%	ON	n/a
Base case + reduced connected pore volume	Reduced PV, V32, single fracture seed, top perf, YM LOW, LTE LOW + 5 years	1.61E+06	1.20E-05	5	Base Case	0.22	0.67	0	14.696	0.778	14.696	0.807	14.696	1.02	100%	ON	YES
WORST CASE: High case kv/kh, reduced PV, no cement above perfs, Skin = 30	Reduced PV, V33, single fracture seed, top perf, YM LOW, LTE LOW + 5 years	1.61E+06	1.20E-05	30	High Case	0.22	0.67	0	14.696	0.778	14.696	0.807	14.696	1.02	100%	ON	YES
WORST CASE: High case kv/kh, reduced PV, no cement above perfs, Skin = 30, high YM & LTE coeff	Reduced PV, V34, single fracture seed, top perf, YM HIGH, LTE HIGH + 5 years	3.20E+06	1.50E-05	30	High Case	0.22	0.67	0	14.696	0.778	14.696	0.807	14.696	1.02	100%	ON	YES
WORST CASE: High case kv/kh, reduced PV, no cement above perfs, Skin = 30, high YM & LTE coeff	Reduced PV, V35, single fracture seed, top perf, YM HIGH, LTE HIGH + 5 years: shut-in well #1, remaining wells inject 1 MMTPA (52 MMscf/d)	3.20E+06	1.50E-05	30	High Case	0.22	0.67	0	14.696	0.778	14.696	0.807	14.696	1.02	100%	ON	YES
Reference Case +	V36, single fracture seed, top perf, YM LOW, LTE LOW + 5 years: shut-in well #1, remaining wells inject 1 MMTPA (52 MMcf/d)	1.61E+06	1.20E-05	5	Base case	0.22	0.67	0	14.696	0.778	14.696	0.807	14.696	1.02	100%	ON	YES
Reference Case +	V38, single fracture seed, top perf, YM VERY LOW, LTE LOW + 5 years: V LOW YM, Skin = 30	8.00E+05	1.20E-05	30	Base case	0.22	0.67	0	14.696	0.778	14.696	0.807	14.696	1.02	100%	ON	YES
Reference Case +	V38, single fracture seed, top perf, YM VERY LOW, LTE LOW + 5 years: V LOW YM, Skin = 5	8.00E+05	1.20E-05	5	Base case	0.22	0.67	0	14.696	0.778	14.696	0.807	14.696	1.02	100%	ON	YES
Reference Case +	V39, single fracture seed, top perf, YM LOW, LTE LOW + 5 years: Fracture conductivity = 1/10 base case	1.61E+06	1.20E-05	5	Base case	0.22	0.67	0	14.696	0.778	14.696	0.807	14.696	1.02	100%	ON	YES
Reference Case +	V40, single fracture seed, top perf, YM LOW, LTE LOW + 5 years; Biot coeff = 1.0	1.61E+06	1.20E-05	5	Base case	0.22	1	0	14.696	0.778	14.696	0.807	14.696	1.02	100%	ON	YES
Reference Case +	V41, single fracture seed, top perf, YM LOW, LTE LOW + 5 years; LOW kv/kh	1.61E+06	1.20E-05	5	LOW case	0.22	0.67	0	14.696	0.778	14.696	0.807	14.696	1.02	100%	ON	YES

List of sensitivity simulations

Table 3: List of sensitivity cases run for the REVEAL™ modelling study.

Table 4 – List of numerical results

Version	Problem with run?	Fracture occurring	Fracture full width	Date fracturing occurs	Average injectivity	Topmost layer reached by fracture
			ft		MMscf/d/psi	
11		YES	499	01/01/2025	0.49	13
12	Re-run with single well skin=5	YES	61	01/03/2039	0.36	20
13		YES	495	01/02/2025	0.45	13
14	Re-run with single well skin=5	YES	18	01/09/2044	0.28	19
15		YES	502	01/02/2025	0.53	12
16	NaN in Jan 2048	YES	n/a unstable fracture calc	01/04/2039	0.24	20
17		YES	341	01/02/2025	0.5	13
18		YES	n/a unstable fracture calc	01/12/2044	0.26	20
19		YES	23	01/01/2044	0.3	20
20		YES	11	01/06/2046	0.27	20
21		YES	160	01/07/2025	0.24	16
22	NaN in Dec 2048	YES	12	01/11/2045	0.37	20
23		YES	117	01/03/2026	0.29	16
24		NO	0	n/a	0.38	n/a
25	NaN in Dec Oct 2034	NO	0	n/a	0.16	n/a
26		NO	0	n/a	0.08	n/a

Table 4 – List of numerical results - continued

Version	Problem with run?	Fracture occurring	Fracture full width	Date fracturing occurs	Average injectivity	Topmost layer reached by fracture
			ft		MMscf/d/psi	
27		NO	0	n/a	0.35	n/a
28		NO	0	n/a	0.23	n/a
29	NaN in Apr 2048	NO	0	n/a	0.08	n/a
30		YES	40	01/11/2042	0.29	21
31		YES	35	01/05/2041	0.32	21
32		NO	0	n/a	0.34	n/a
33		YES	169	01/03/2026	0.29	14
34		YES	567	01/01/2025	0.45	10
35		YES	550	01/02/2025	0.51	10
36		YES	80	01/11/2038	0.22	19
37		NO	0	n/a	0.1	n/a
38	Stopped Oct 2034 Nan	NO	0	n/a	0.16	n/a
39		YES	18	01/04/2046	0.25	19
40		NO	0	n/a	0.23	n/a
41		YES	10	01/07/2048	0.12	20

Table 4: List of numerical results per version of the simulation runs (cont'ed)

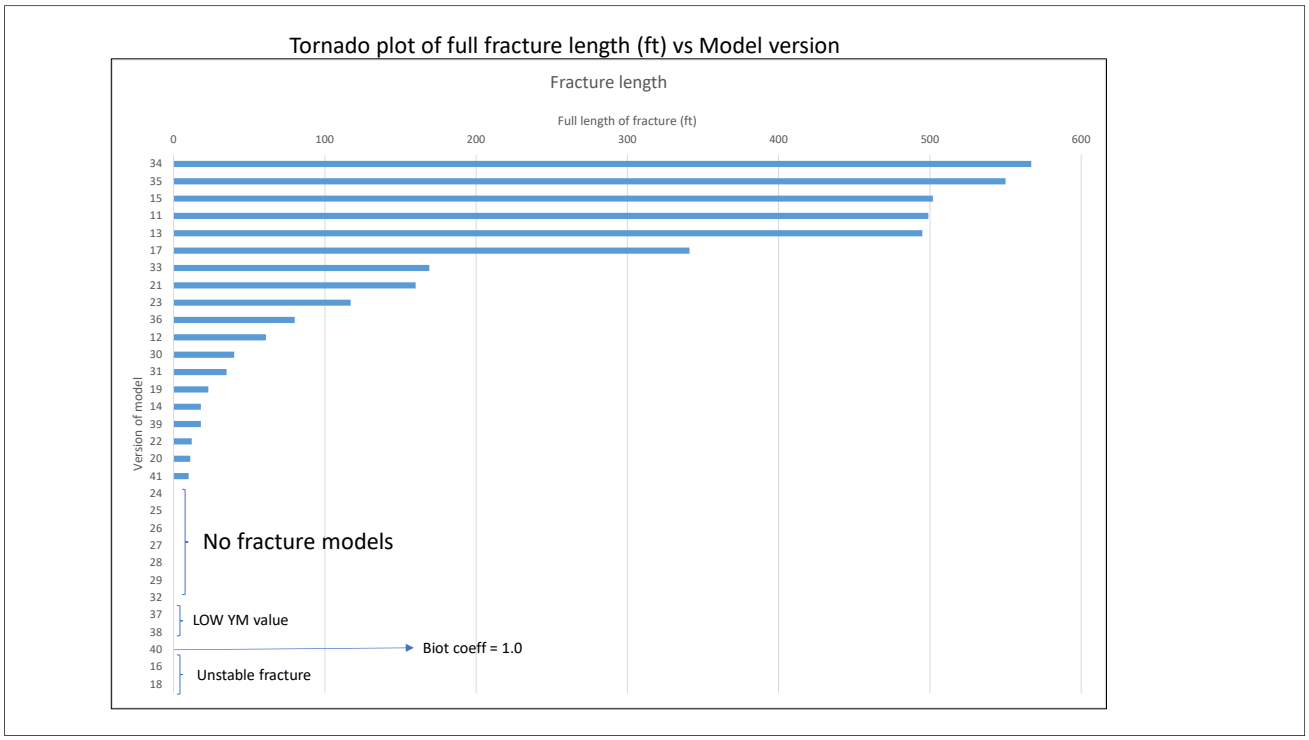

Figure 18: Full fracture length vs simulation version number

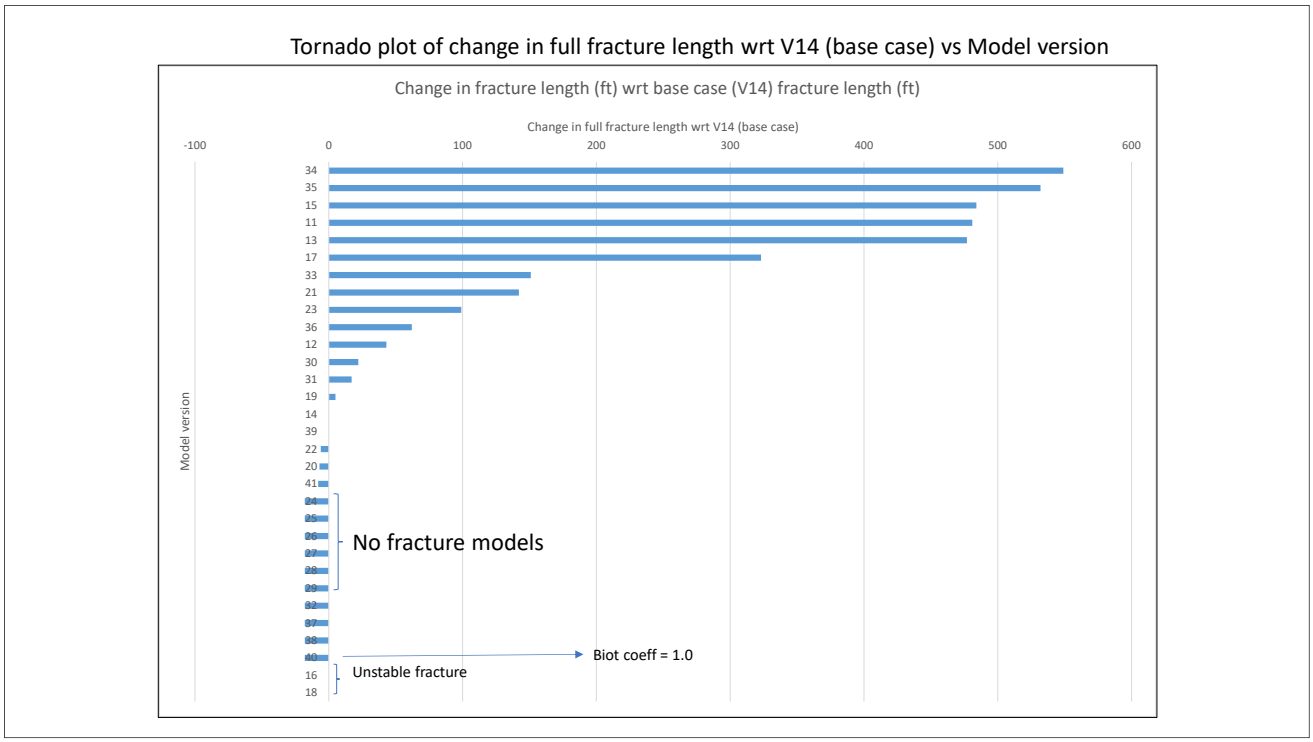

Figure 19: Change in full fracture length, with respect to the base case (V14)

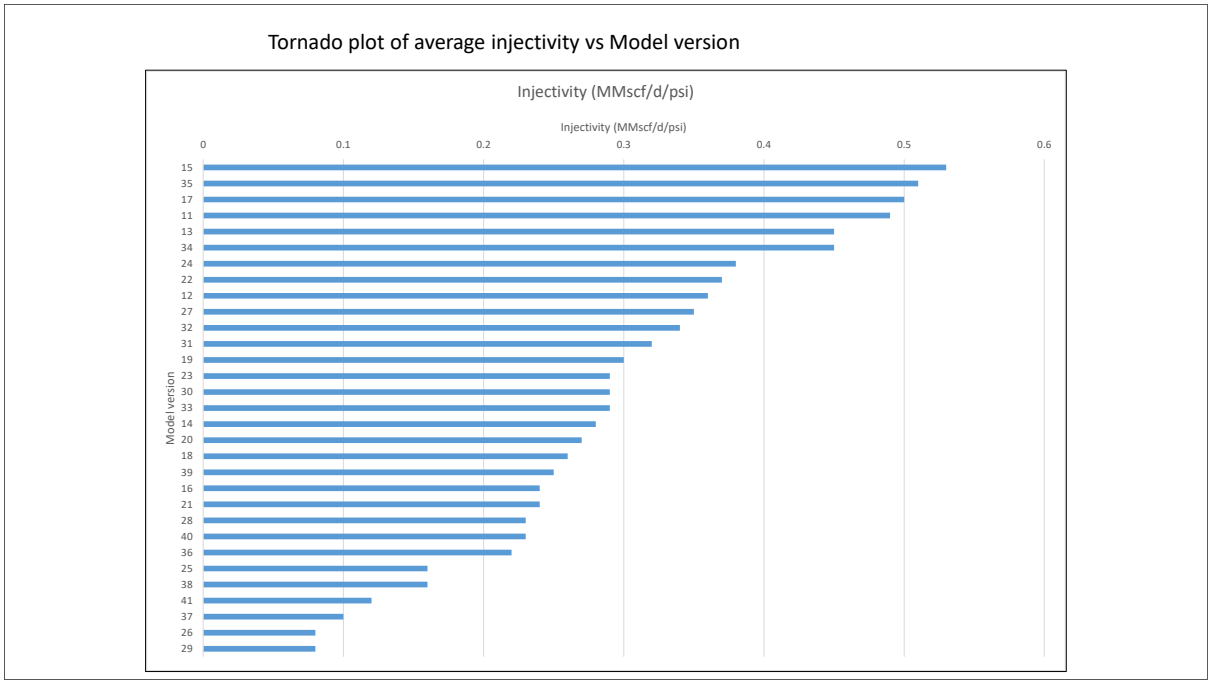

Figure 20: Average injectivity vs simulation version number

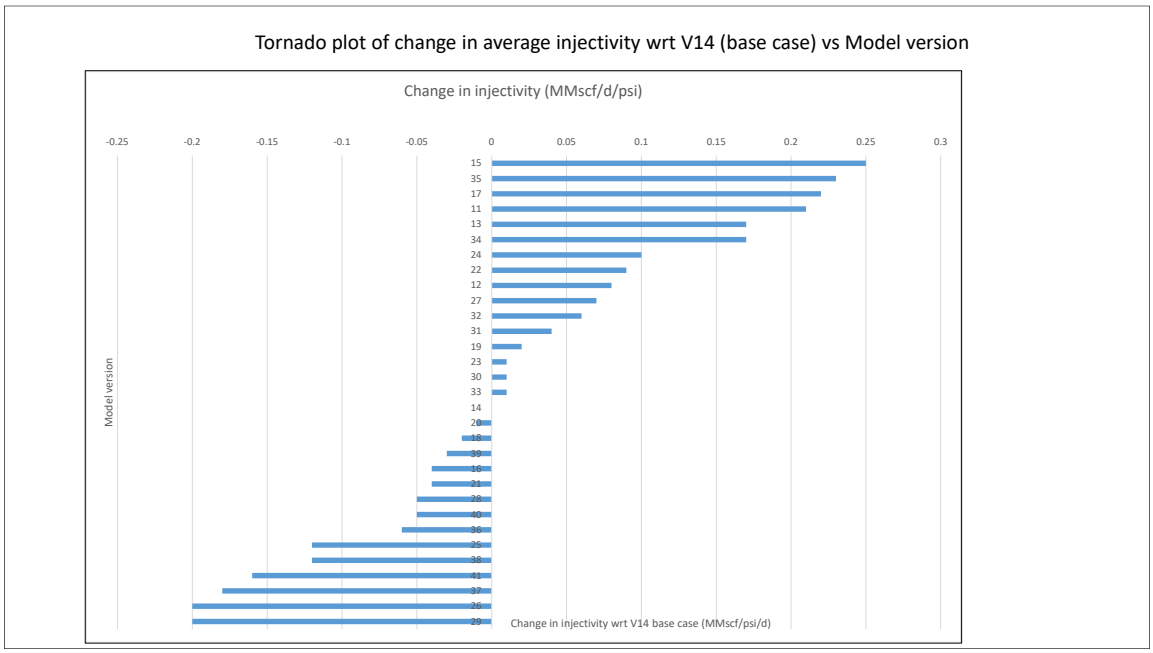

Figure 21: Change in average injectivity versus simulation version number

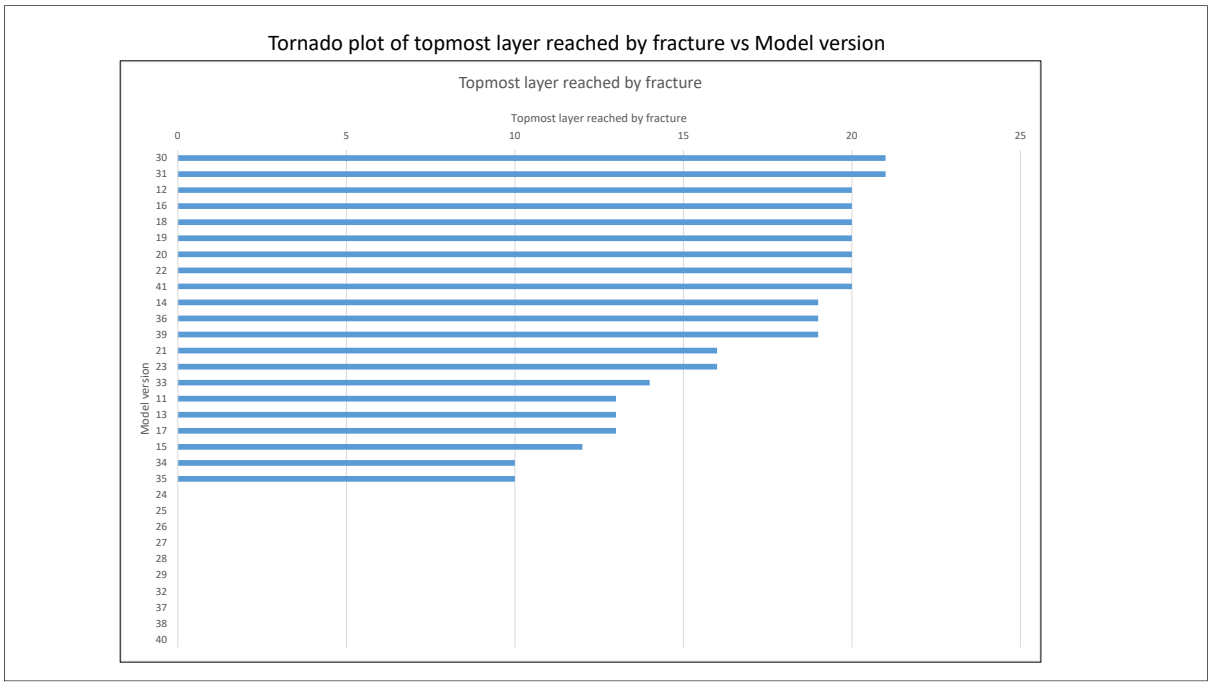

Figure 22:Topmost layer reached by fracture versus simulation version number

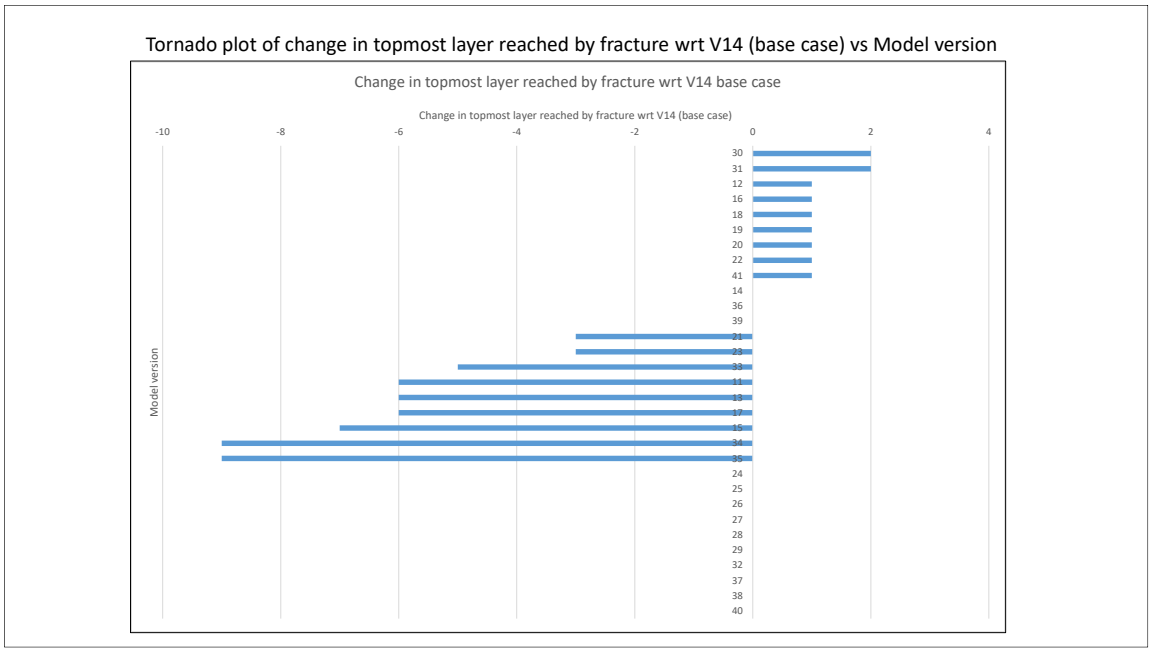

Figure 23: Change in topmost layer reached by fracture versus simulation version number

Tornado plot of change in start time of fracture wrt V14 (base case) vs Model version

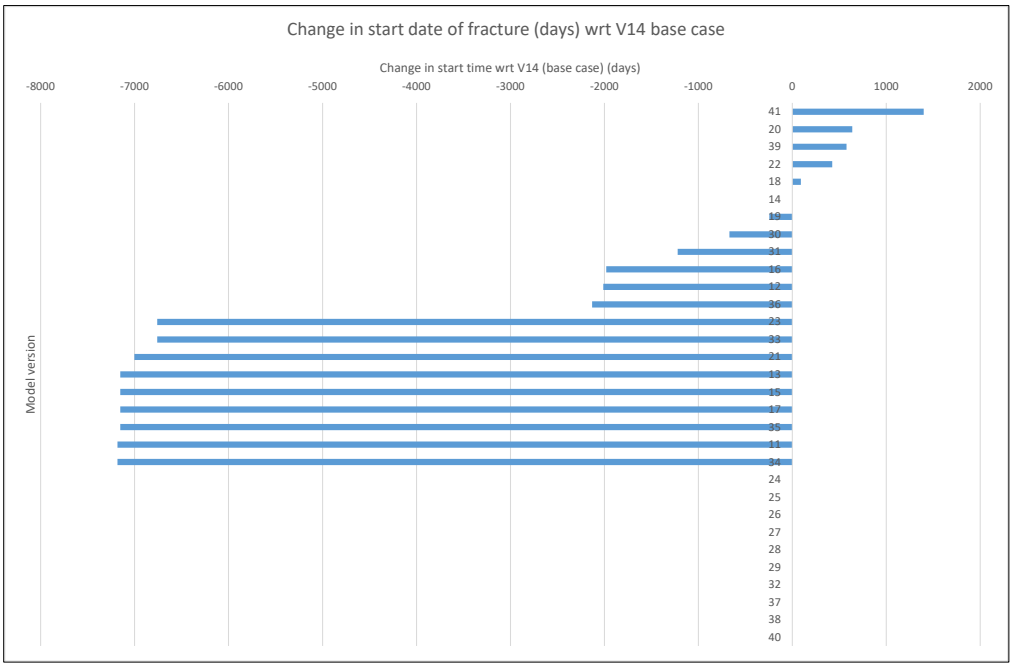

Figure 24: Change in start time of fracture versus simulation version number

8.0 Interpretation of the Results

8.1 Mechanism of Fracture Formation and CO2 Conformance

Fracturing occurs when the cool injected CO2 reduces the effective stress in the formation close to the flowing perforations by increasing the pore pressure and decreasing the temperature. When the effective stress becomes sufficiently negative the rock fractures, increasing the flow rate in the fractured perforated interval which further pressurises and cools the formation, leading to further fracture growth. This continues until the effective stress at the fracture tip is balanced by the rock strength. (The pore pressure is lower at the tip than at the perforation and the temperature is higher.) The growth of the fracture and the flow rate through it are positively coupled; one reinforces the other. The effect is to increase the length of a fracture but to restrict its growth vertically. The more fluid flowing horizontally through fracture, the less fluid remains in the well to flow out through deeper perforations. This can be seen in Figure 25 where the CO2 saturation at the end of the injection period is larger at deeper intervals in the base case (V14) than in the case with the largest fracture, V34. Both images show a positive correlation between high CO2 saturations (red) and the widest part of the fracture.

Although there is vertical growth of the fracture above the initial seed point (layer K = 20) in some cases, in none of them does the fracture ascend out of the Bunter sandstone. The shallowest fractures occur in V34 and V35, the “worst” cases. Even here, the fracture only

rises to layer K = 10. We were unable to create a case where the fracture moved into the caprock. We therefore consider this to be an unlikely event.

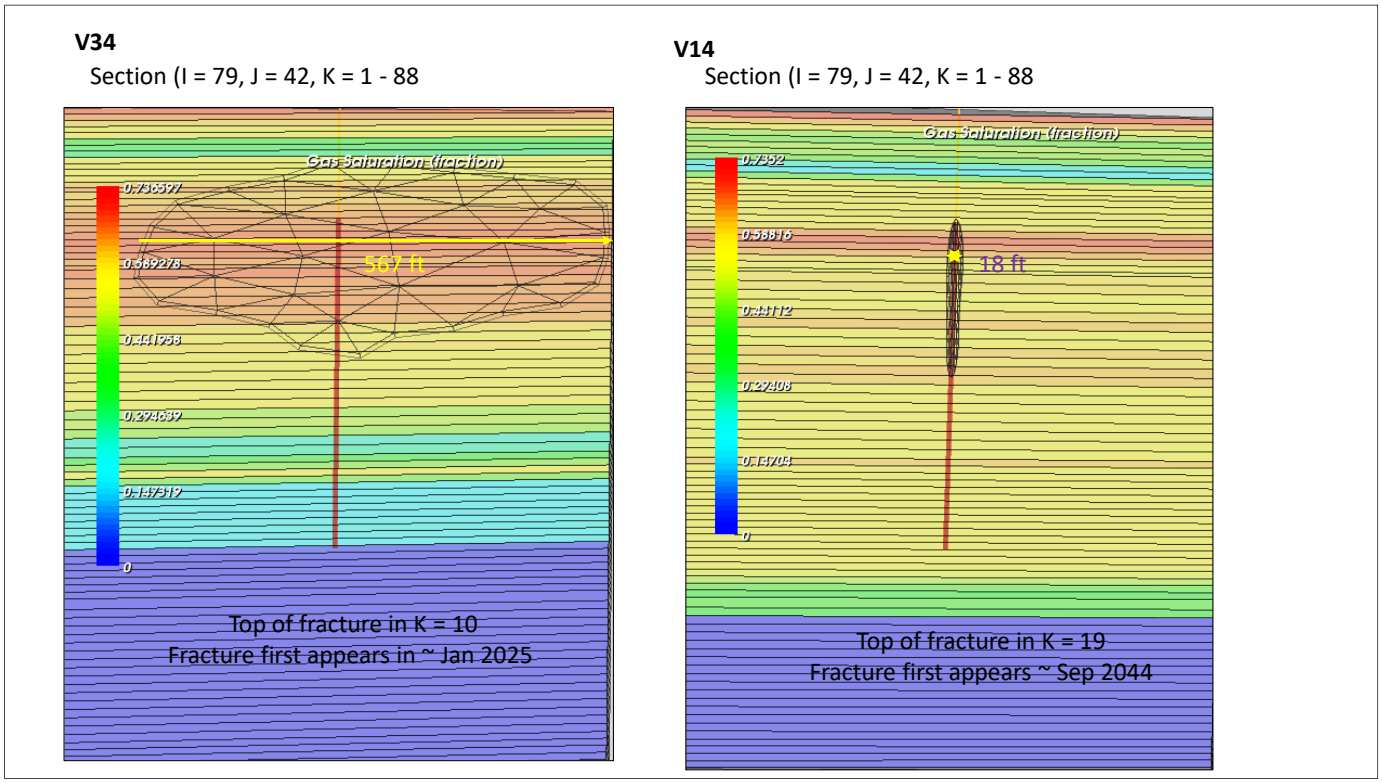

Figure 25: Comparing the CO2 saturated intervals at the end of injection in V34 and V14

8.2 Effect of Each Parameter on Thermal Fracturing

8.2.1 Young's Modulus (YM)

There is a clear positive correlation, or association, between larger values of Young's modulus and large fractures. For example, in the cases of the largest fractures, V34 (576 ft) and V35 (550 ft), "worst" case combinations of parameters, Young's modulus took its largest tested value. For the mid case value, the largest fracture occurred for V33, a "worst" case combination of parameters where the fracture length was 169 ft.

Fractures did not occur when we used the smallest value of Young's modulus tested, V37 and V38. It is noticeable that after V34 and V35, the next three largest fractures, V15 (502 ft), V11 (499 ft) and V13 (495 ft) all have the high value of Young's modulus.

8.2.2 Linear Thermal Expansion Coefficient (LTEC)

As with Young's modulus, there is a positive association between the large value of this parameter and large fracture lengths as thermal stress reduction is proportional to the product of the Young's modulus and the linear thermal expansion coefficient.

The two largest fractures, V34 and V35, occurred with the large value of this parameter.

When we used its small value, together with the small value of Young's modulus, in a combination of other parameters designed to create a worst case, V33, the fracture length fell from ~ 550 ft (V34 and V35) to 169 ft.

After V34 and V35, the next three largest fractures, V15 (502 ft), V11 (499 ft) and V13 (495 ft) all have the high value of Young's modulus. V15 and V11 take the high value of the LTEC and V13 takes the low value.

Low values of Young's modulus are associated with smaller fracture lengths irrespective of the value of the LTEC, for example V12 and V14 (base case)

Working together, Young's modulus and the LTEC parameters, have a strong effect on the size of the fracture.

8.2.3 kv/kh Ratio (Reservoir Architecture)

The three geological models for Endurance were considered as low, mid and high cases.

It has a less clear-cut effect on the fracturing. This is possible not so surprising because it is a large-scale parameter and fracturing is something more likely to be affected by parameters close to the well, unless the large-scale parameter has a significant effect locally to the well.

For example, two low mid case kv/kh cases, V11 (499 ft fracture length) and V13 (495 ft fracture length) may be compared their equivalent high case kv/kh cases, V15 (502 ft fracture length) and V17 (341 ft fracture length) respectively. There is no obvious trend here as there is with Young's modulus.

V41 had a low value of kv/kh. The fracture length was 10 ft, compared with 18 ft in the base case. The average injectivity was 0.12 MMscf/d/psi compared with 0.28 MMscf/d/psi in the base case.

8.2.4 Degree of Cementation Above the Well

These cases were V19 (otherwise a copy of the base case, V14), and V33, V34 and V35 ("worst" cases).Figure 26 compares the final fracture shapes for V19 and V14.

This parameter seems to make only a little difference. The fracture is slightly longer and deeper in V19 and it has a slightly higher average injectivity (0.3 MMscf/day/psi compared with 0.28 MMscf/d/psi).

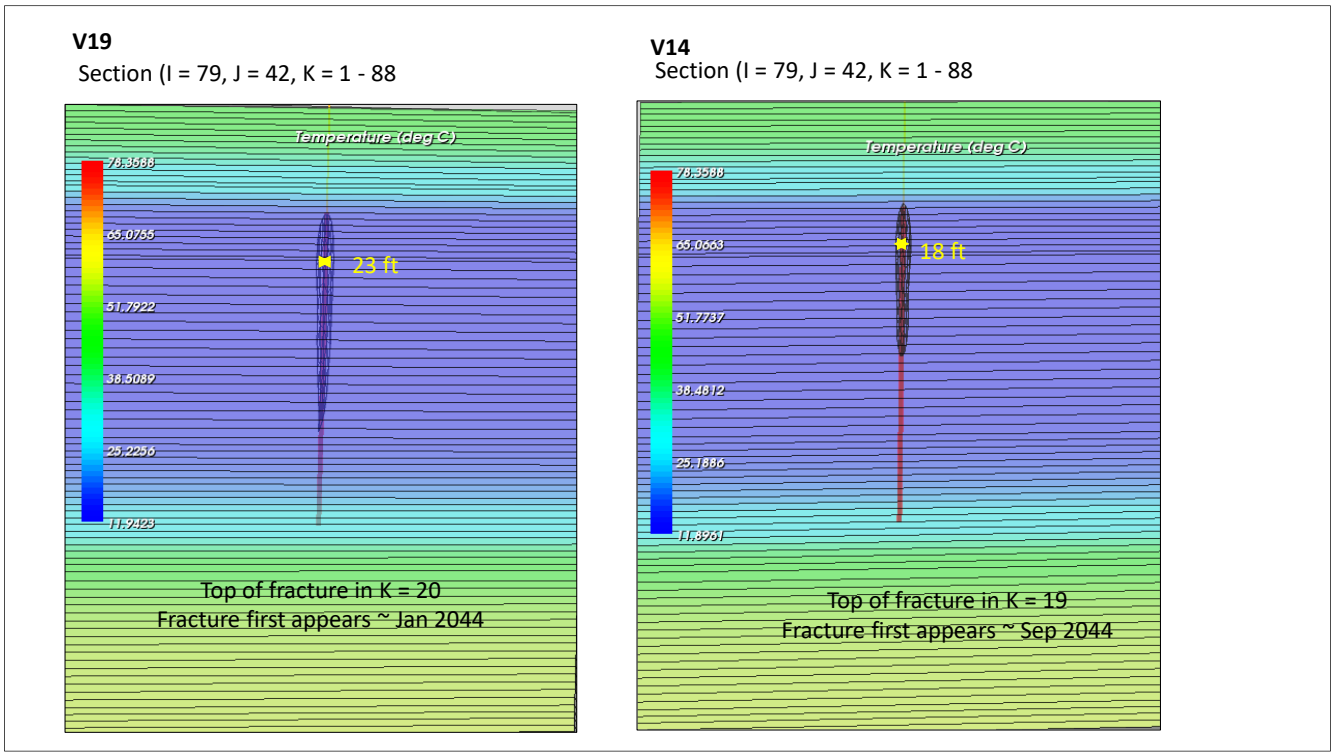

Figure 26: Comparing V19 (no cemented layer above well) and V14 (cemented layer above well)

The effect of the cemented layer above the well seems to increase the pore pressure allowing the fracture to grow to a shallower depth in V14, and to be longer at shallower depths. In contrast, in V19 the fracture grows deeper as the pore pressure increases there with deeper injection. However, the effect is small, compared with changes in Young's modulus for example.

8.2.5 Well Skin

The skin has a strong effect on the size of the fracture, for example compare V20 (skin = 0), V14 (skin = 5) and V21 (skin = 30). All the other parameters are unchanged. The fracture length in V20 is 11 ft, in V14 it is 18 ft and in V21 it is 160 ft.

In another series of runs where the kv/kh ratio was set to its high value, three comparable runs have been generated: V22 (skin = 0), V18 (skin = 5) and V23 (skin = 30). The corresponding fracture lengths were 12 ft, (n/a, unstable fracture growth) and 117 ft.

Clearly there is a positive association between a large skin and a large fracture, for obvious reasons. The effect is stronger than those created by changing the kv/kh ratio and the presence, or not, of a cemented layer above the well.

8.2.6 Connected Pore Volume

The connected pore volume was reduced by a factor of two in V32 (otherwise a copy of the base case), V33 (a worst case), V34 (a second of worst cases) and V35 (third of worst cases).

We examine V32 because it is easier to analyse this case as there are fewer varying parameters.

Figure 27 shows the fracture at the end of injection. It is a very thin (~ 1 ft) fracture which has gone deep into the formation. One might expect a larger fracture than in the base case because the pore pressure would be larger but it is difficult to explain the shape of the resulting fracture in this case.

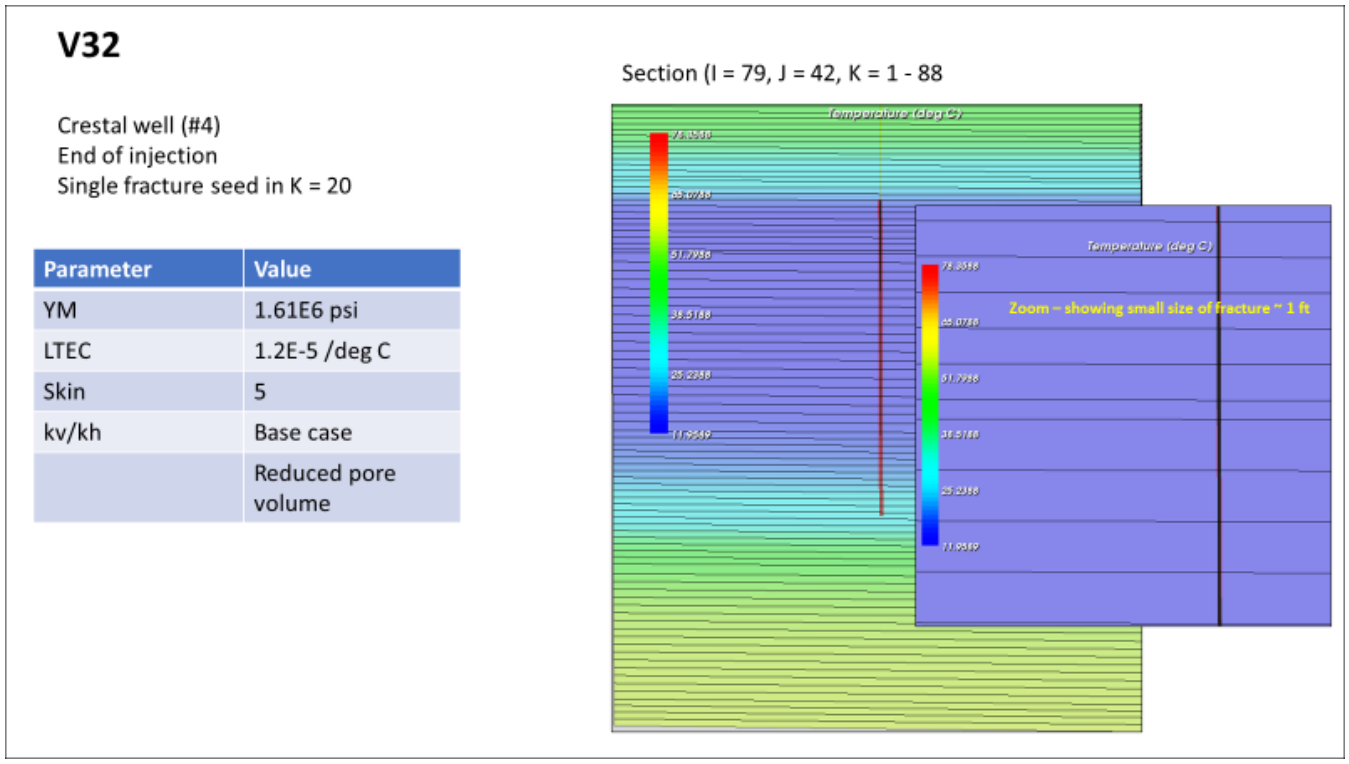

Figure 27: V32 copy of base case with half connected pore volume

8.2.7 Number of Fracture Seeds

The number of fracture seeds was increased from one in the base case, to two in V30 and three in V31. In V30, seed fractures were placed in layers K = 20 and 30; and in V31 they were placed in layers K = 20, 30 and 40.

Figure 28 shows the resulting fractures in V30 and V31.

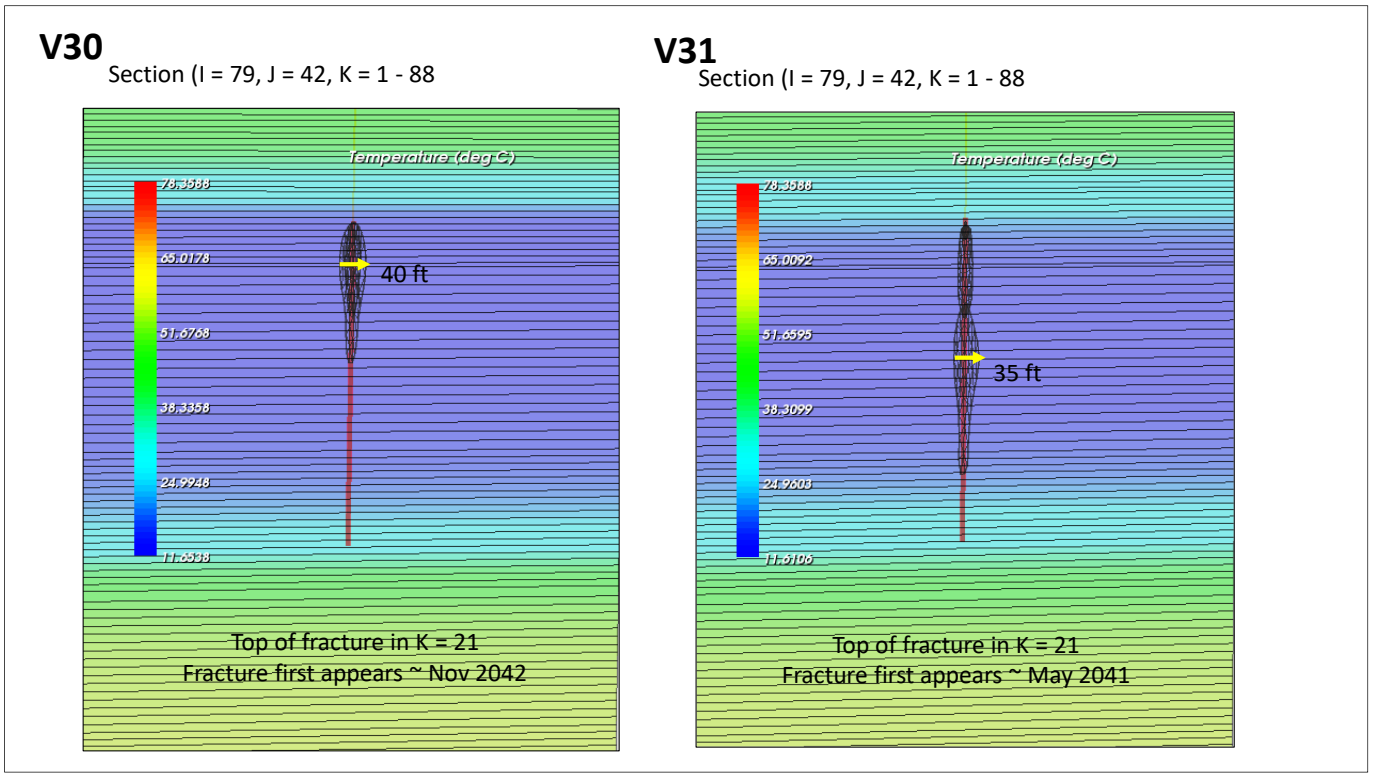

Figure 28: V30 (2 seeds) and V31 (3 seeds)

The results show that multiple fractures are possible but that the overall effect of fracture length is small. The average injectivities for the base case (V14), V30 and V31 were 0.28, 0.29 and 0.32 MMscf/d/psi respectively.

8.2.8 Biot Coefficient

In V40, otherwise a copy of the base case, the Biot coefficient was set to 1.0. The effect was to delay the onset of fracturing.

8.2.9 Fracture Conductivity

In V39, the fracture conductivity was reduced by a factor of 10x from 1.0 Dft to 0.1 Dft.

The effect is shown in figure 28, where the resulting fracture is of equal length to that in the base case (V14) nut about half the height. The average injectivity is 0.25 MMsf/d/psi in V39, compared with 0.28 MMscf/d/psi in the base case. Figure 30 shows the estimation of the pressure gradient within the fracture in V39. The horizontal pressure gradient is ~ 1.1 psi/ft compared with ~ 0.4 psi/ft in the base case. At deeper depths the tip pressure in V39 is insufficient to cause fracturing.

V39

Crestal well (#4)
End of injection
Single fracture seed in K = 20

Parameter	Value
YM	1.61E6 psi
LTEC	1.2E-5 /deg C
Skin	5
kv/kh	Base case
	Frac conductivity = 1/10 base case

Section (I = 79, J = 42, K = 1 - 88

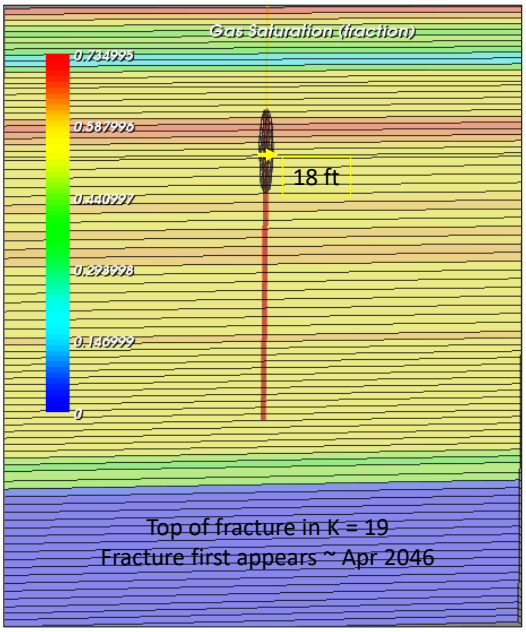

Figure 29: V39 fracture at the end of injection

V39

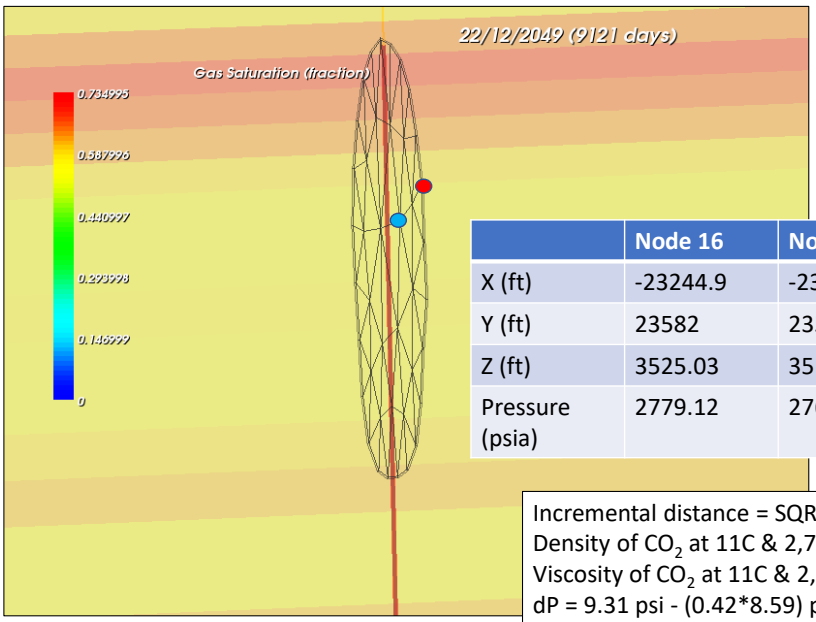

Node 9
Node 16

	Node 16	Node 9	Increment	
X (ft)	-23244.9	-23242.7	2.2	
Y (ft)	23582	23586.8	-4.8	
Z (ft)	3525.03	3516.44	8.59	
Pressure (psia)	2779.12	2769.81	9.31	

Incremental distance = SQRT(2.2^2 + 4.8^2) = 5.28 ft
Density of CO_2 at 11C & 2,770 psia ~ 970.6 kg/m3 = 0.42 psi/ft
Viscosity of CO_2 at 11C & 2,770 psia ~ 0.11 cP
dP = 9.31 psi - (0.42*8.59) psi = 5.7 psi
dP/d$\underline{X}$ = ~ 1.1 psi/ft within fracture

Figure 30: V39 - calculation of pressure gradient within the fracture

8.3 Cases to Illustrate Effect of Parameters

To illustrate the effects of the parameters four cases were considered in greater details: V14 (the base case), V34 (the largest fracture case), V15 (third largest fracture case) and V37 (hard to fracture, low injectivity case). Table 5 lists the four cases.

Results of 4 cases

Case	Description	Model version	YM (psi)	LTE ($^oC^{-1}$)	kv/kh	Skin	Cement above well	Connected PV
1	Base case	V14	Mid	Mid	Mid	5	Yes	Mid
2	Largest fracture	V34	High	High	High	30	No	Low
3	2'nd largest fracture	V15	High	High	High	5	Yes	Mid
4	Hard to fracture – low injectivity	V37	Low	Mid	Mid	30	Yes	Mid

Table 5: Four cases to illustrate the effect of changing the parameters

- Case 1: V14 (base case) has mid-case values for Young's modulus and the LTEC. The skin is 5 (mid case), and the kv/kh ratio is mid-case. The connected pore volume is the base case value. There is a cemented layer above the well.
- Case 3: V15 has high values for Young's modulus and the LTEC. The skin is 5, and the kv/kh ratio is high. The connected pore volume takes the base case value. There is a cemented layer above the well.

So V14 and V15 are identical except for the differences in Young's modulus and the LTEC.

- Case 2: V34 is one of the "worst" (high risk?) case examples. It has high values for Young's modulus and the LTEC. The skin is 30, and the kv/kh ratio is high. The connected pore volume is low. There is no cemented layer above the well.
- Case 4: V37 has the low value for Young's modulus and the low value for LTEC. The skin is 30, and the kv/kh ratio takes the base case value. The connected pore volume takes the base case value. There is a cemented layer above the well. It represents a low risk case for fracturing but is therefore at a higher risk of having an injectivity which is too low.

Figure 31 and Figure 32 show the temperature and CO2 saturation at the end of injection in the four cases. They clearly show how the gas saturation and temperature distribution conform

the fracture height, when a fracture has occurred. In the absence of a fracture the whole perforation length is used.

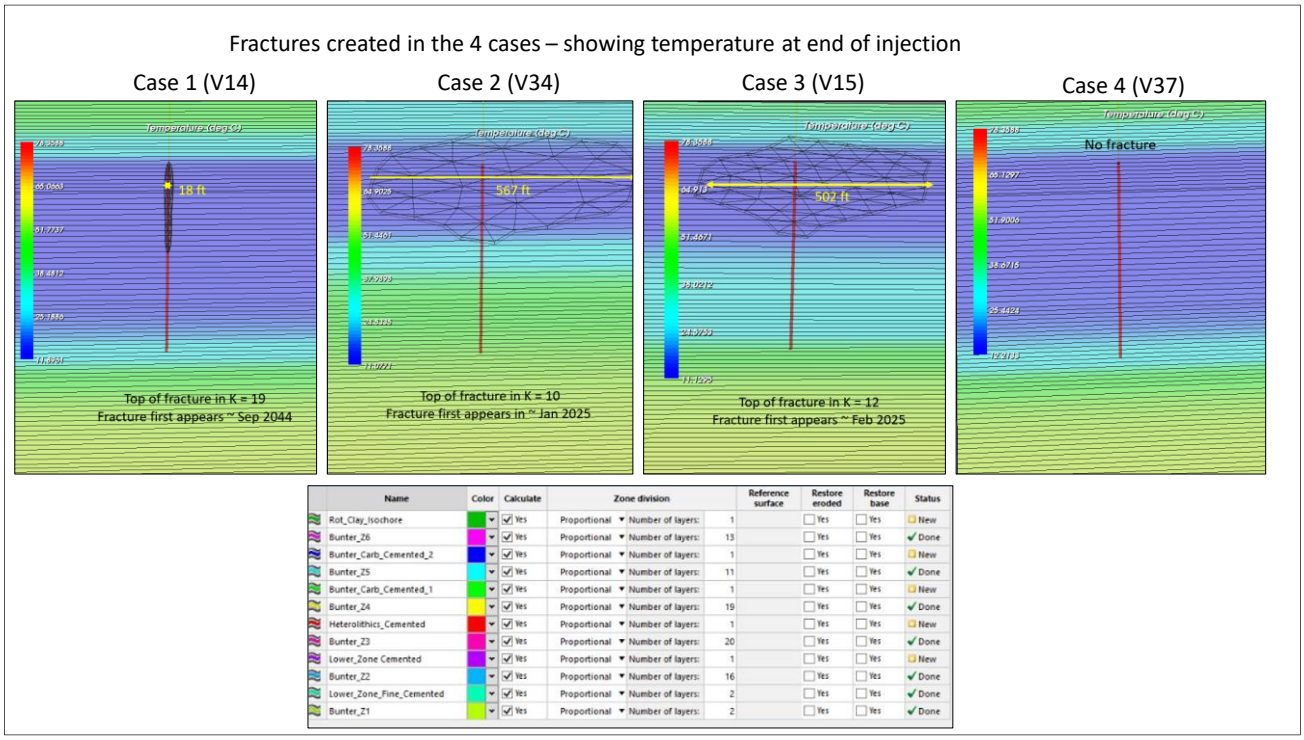

Figure 31: Temperatures at the crestal well in the four cases, end of injection

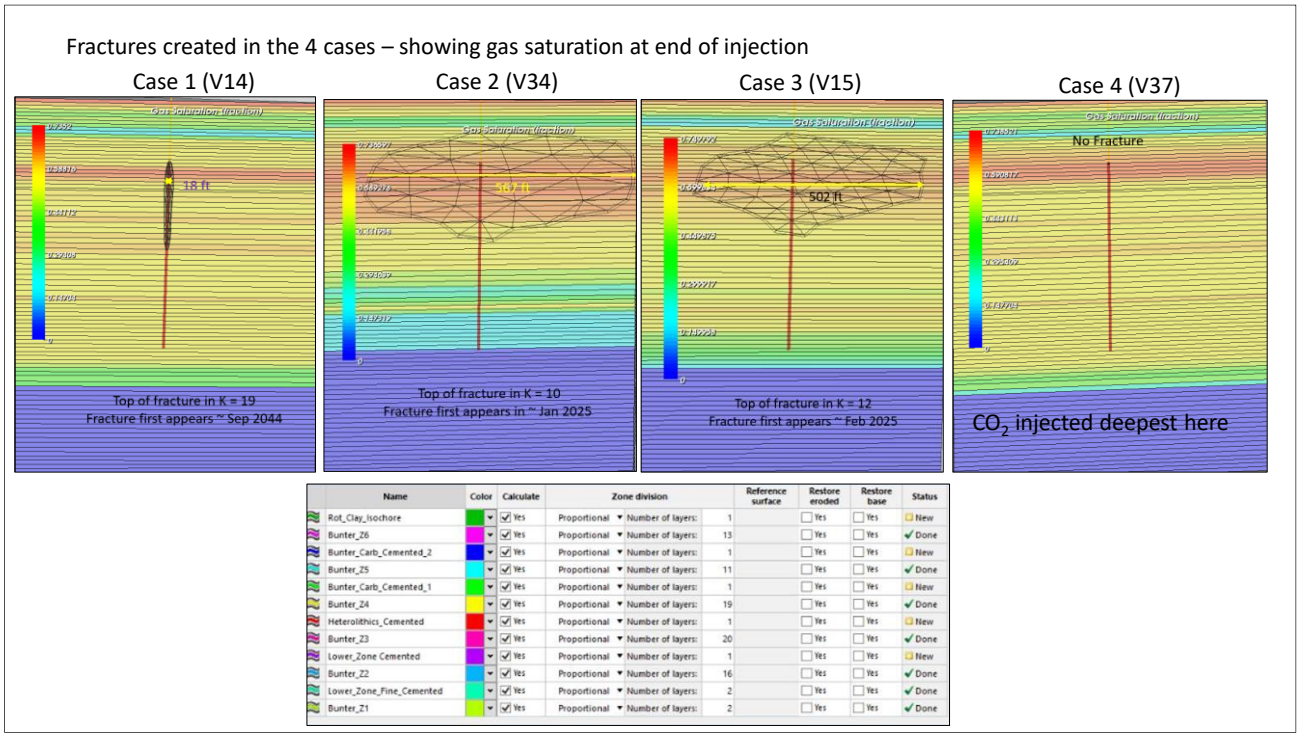

Figure 32: Gas saturations at the crestal well in the four cases, end of injection

Figure 33 and Figure 34 compare the injectivities for the four cases, the BHPs, reservoir pressures and plot the safe BHP. It also shows that the apparent major contribution to a large fracture is a high Young's modulus coupled with a large LTEC, irrespective of the other parameters.

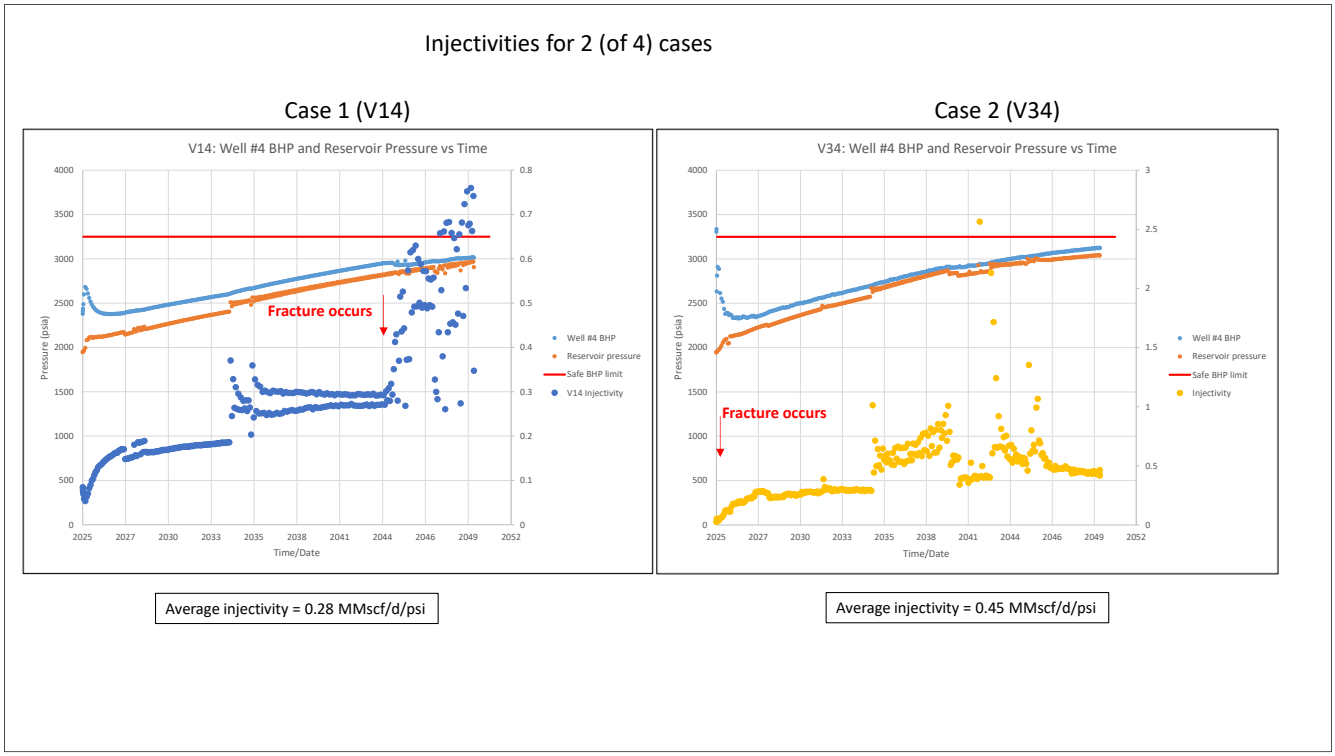

Figure 33: Injectivities for cases 1 (V14) and 2 (V34)

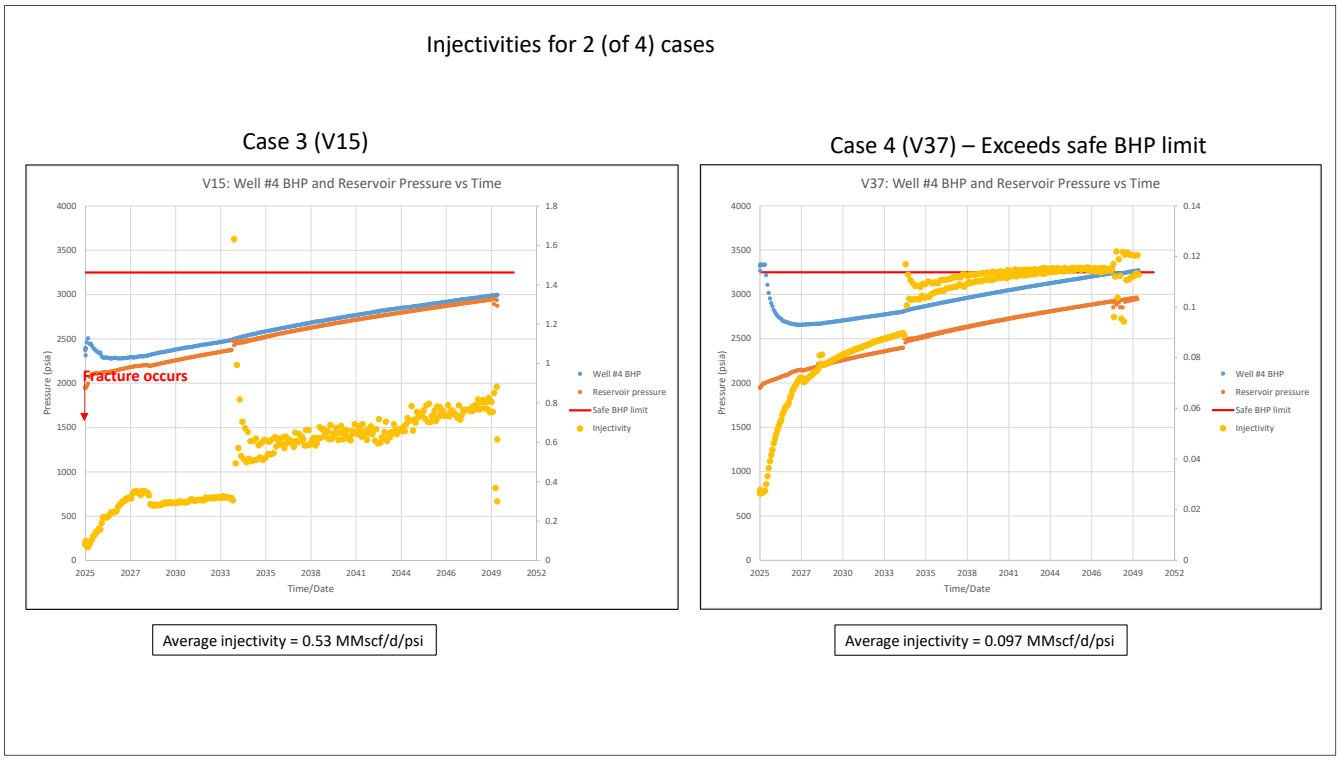

Figure 34: Injectivities for cases 1 and 2.

The case with the largest fracture has an average injectivity (V34) which is 4.5 times greater than the lowest injectivity case (V37). The case with the second largest fracture (V15) has five times as much average injectivity as the lowest (V37).

Figure 35 to Figure 38 show cross sections of gas saturation, at the end of injection, through the model for the four cases. One cross section is taken through the crestal well; the other is through well #3.

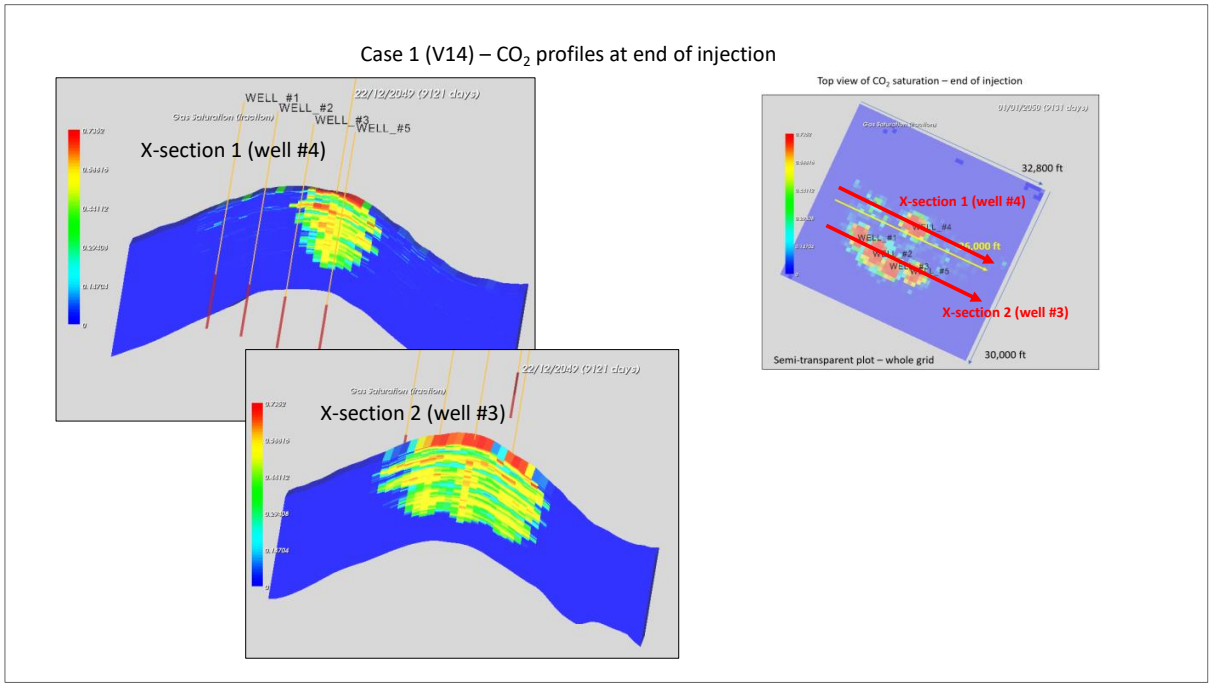

Figure 35: Case 1 (V14) - cross sections through the crestal well and well #3, end of injection

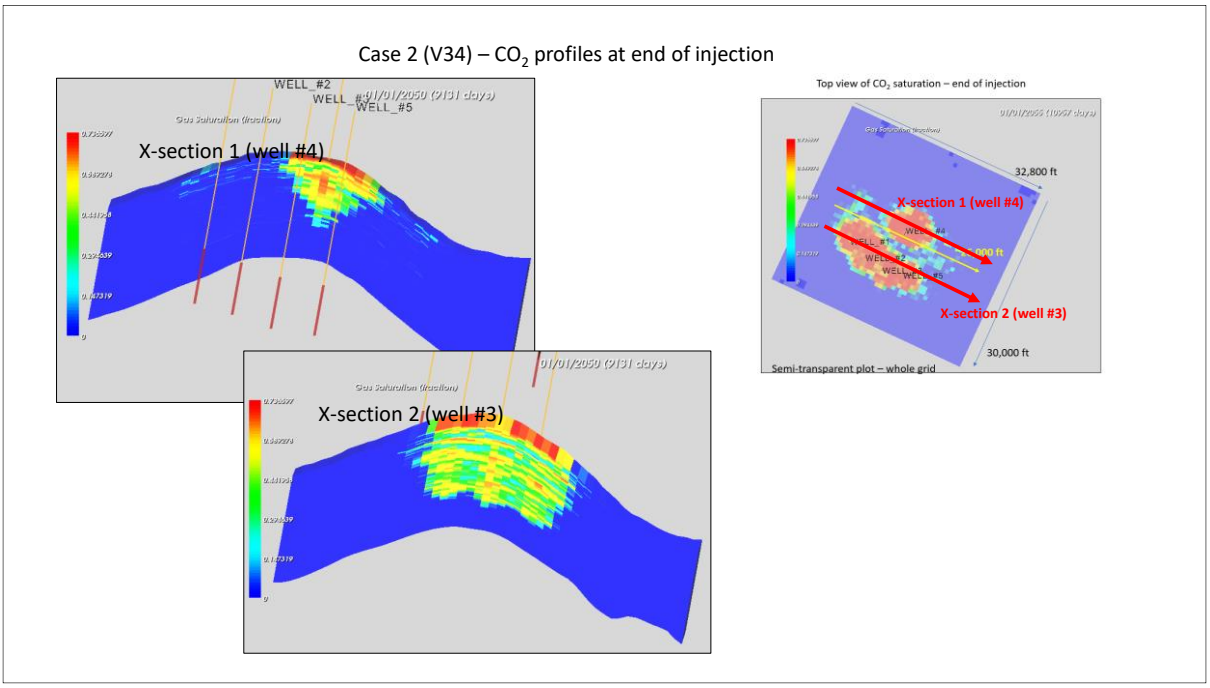

Figure 36: Case 2 (V34) - cross sections through the crestal well and well #3, end of injection

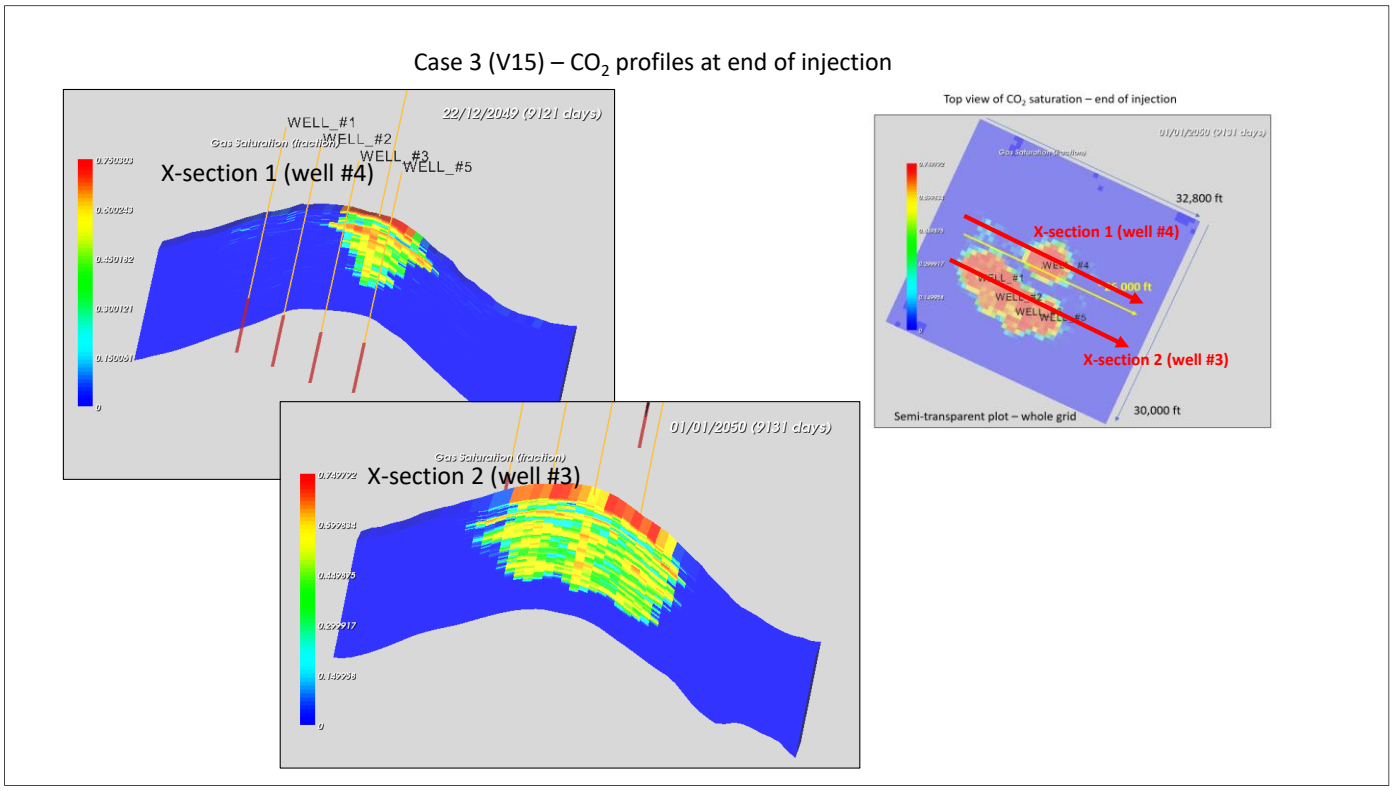

Figure 37: Case 3 (V15) - cross sections through the crestal well and well #3, end of injection

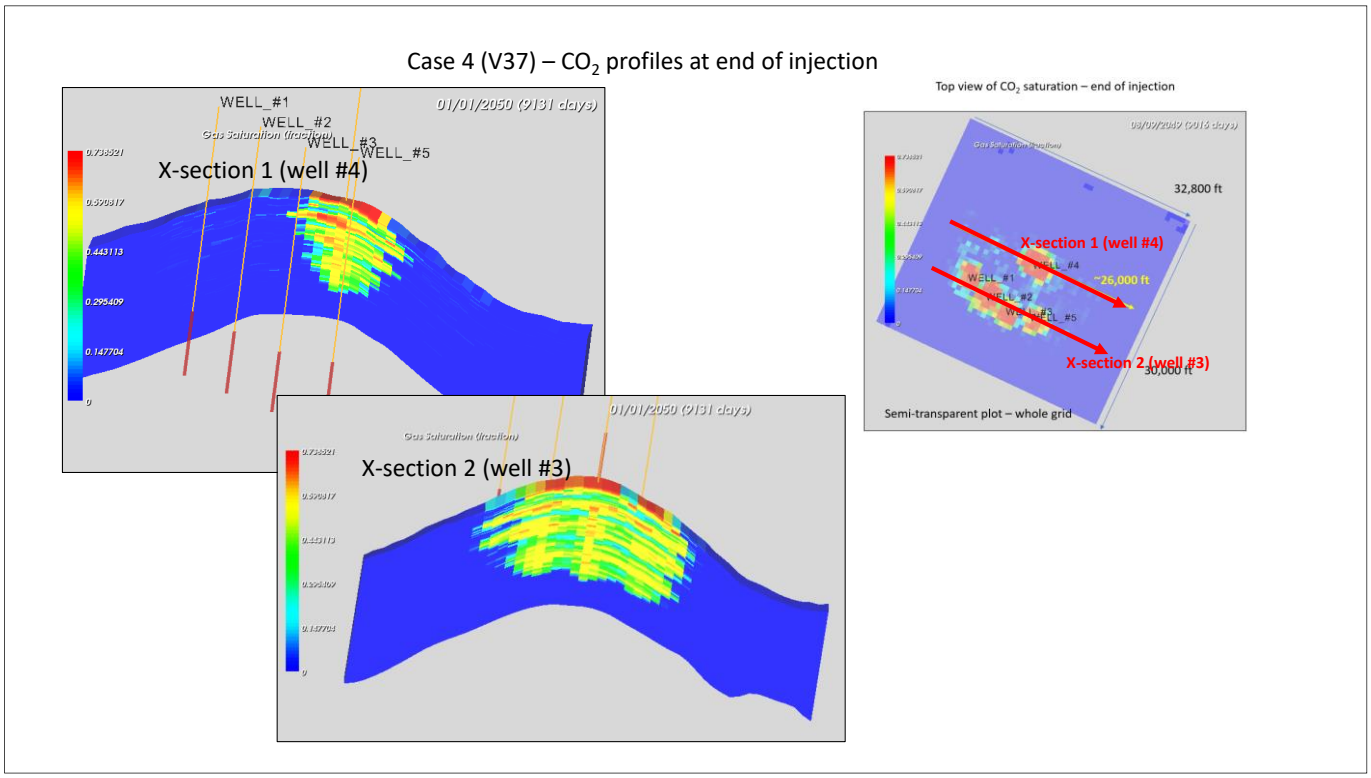

Figure 38: Case 4 (V37) - cross sections through the crestal well and well #3, end of injection

Figure 39 and Figure 40 show the temperature cross sections through the crestal well at the end of injection. The temperature profile is correlated with the shape of the fracture and vice-versa.

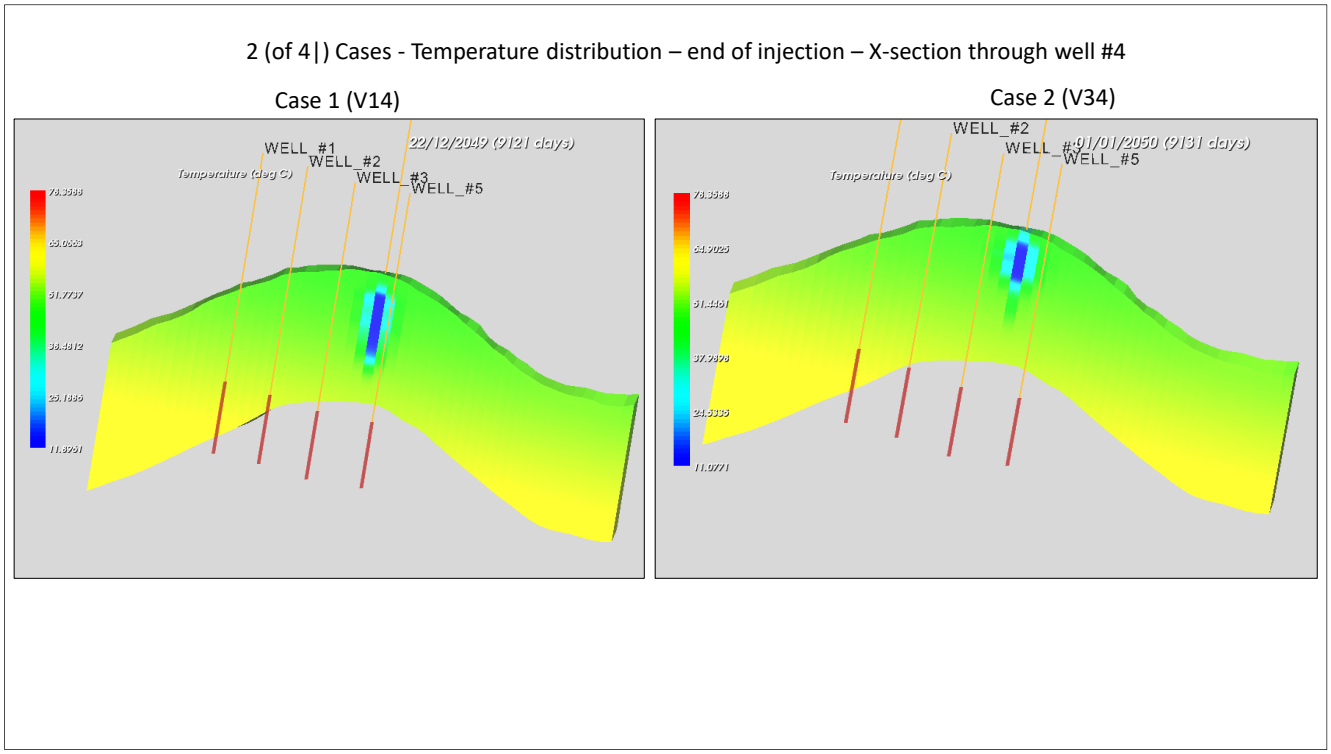

Figure 39: Case 1 (V14) and case 2 (V34) temperature cross sections, end of injection

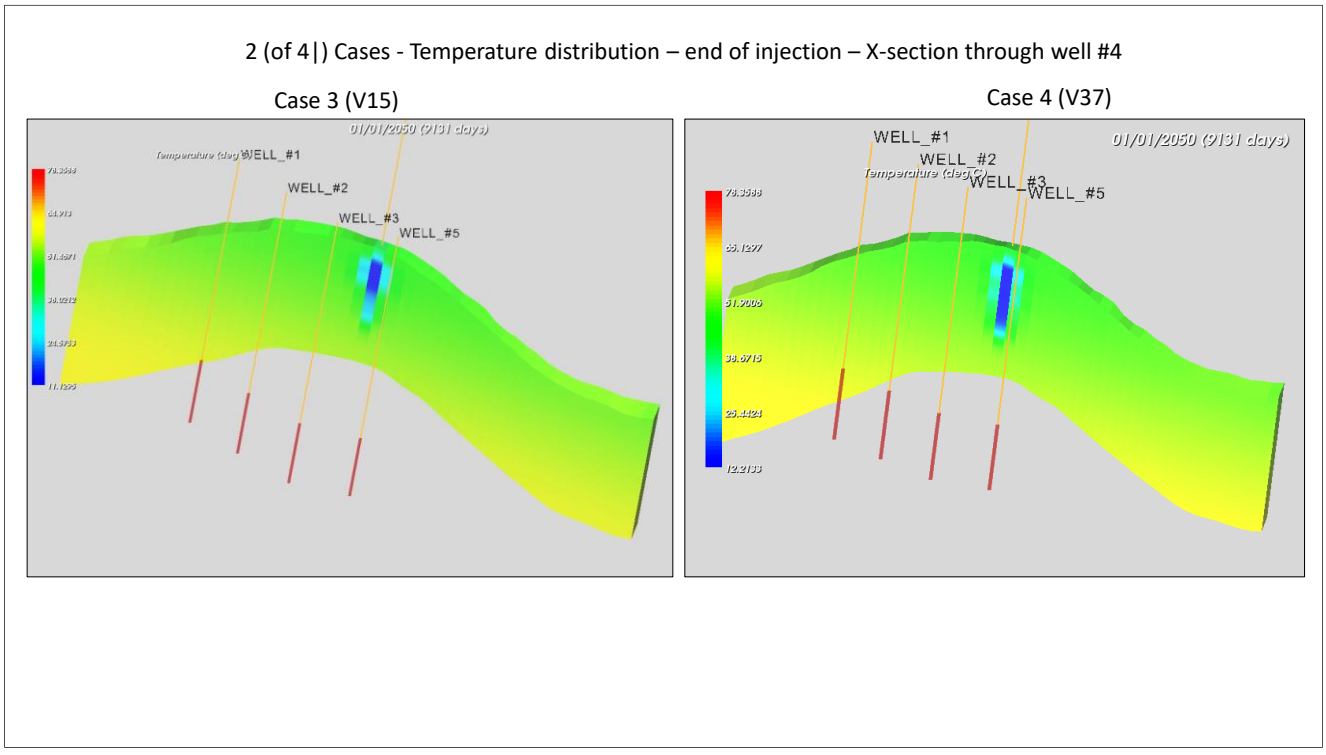

Figure 40: Case 3 (V15) and case 4 (V37) temperature cross sections, end of injection

9.0 Summary of Results

The results of the study have indicated the following:

- The Risk of vertical fracture growth is manageable and low based upon screened tested cases:
    - No case presents fracture reaching top Bunter by the end of injection
    - The study has demonstrated the value of leaving a section of the Bunter unperforated (at least 20-30 meters), both for pressure limit and conformance
- Fractures follow the temperature profiles. The tendency is for positive feedback where cool CO2 reduces the temperature of the formation and fracturing occurs. Then more CO2 flows into the fractures causing more cooling and the process is repeated and enhanced.The most important parameters are the combination of Young's modulus and the LTEC which drive the thermo-elastic stress reduction

- Skin build-up (and associated injectivity loss) is likely to be offset by thermal fracturing. In the low probability case where fracturing does not occur and there is formation damage (case #4/V37 with low Young's Modulus and high skin S=30), late life BHP could require curtailment due to operating pressure limit for the crestal well. This indicates the importance of avoiding high skin in order to achieve acceptable injection rate across the full uncertainty range. Further assurance on Young's modulus would help, for example from quantitative analysis of the 2013 water injection test in 42/25d-3, in which fracturing did occur.

- Thermal fracturing is not adversely impacting the confinement of CO2 plume movement. In particular, it appears to be a low risk of CO2 moving vertically through a fracture to top reservoir. The potential low kv/kh system (well 42/25d-3 PTA interpretation) would support longer perforated interval i.e. 80 meters. The well is unlikely to thermally fracture immediately hence maintaining good conformance over the initial period.

10.0 References

(Petroleum Experts, 2020): Petroleum Experts Limited, Petex House, 10 Logie Mill, Edinburgh, EH7 4HG, United Kingdom; www.petex.com; email: edinburgh@petex.com.

This publication is available from: www.gov.uk/beis

If you need a version of this document in a more accessible format, please email enquiries@beis.gov.uk. Please tell us what format you need. It will help us if you say what assistive technology you use.